Poznan University of Technology
Faculty of Civil and Transport Engineering

Doctoral Dissertation

**Paulina Stempin**

# Structural models in the framework of space-Fractional Continuum Mechanics

Supervisor: Prof. Wojciech Sumelka

# *Acknowledgments*

I would like to express my heartfelt gratitude to my supervisor, Prof. Wojciech Sumelka, for indicating the direction of my research and for his support and mentorship throughout the entire duration of my doctoral research. I appreciate his constant encouragement to take on new scientific challenges, attention to my scholarly growth, and balance between guiding me and allowing me the independence to explore my ideas.

In short, I sincerely thank Prof. Wojciech Sumelka for being an exemplary supervisor.

The research presented in this dissertation was supported by the National Science Centre, Poland under Grant No. 2017/27/B/ST8/00351.

# Contents

# Abstract

The research problem examined in the dissertation concerns modeling of structural elements that exhibit scale effect, e.g. nano- and micro-scale elements. In that case, classical continuum mechanics fails since it does not account for the fact that materials are heterogeneous (e.g. granular, porous) when considered at sufficiently small scales. Scale effect then appears, meaning the impact of heterogeneity of the internal structure on the object's behavior. As a consequence, the characteristic length of the internal structure (length scale) needs to be included when describing body behavior at scales close to the microstructure. The inability of continuum mechanics to account for the scale effects motivated the development of generalized continuum (non-local) theory, i.e. space-Fractional Continuum Mechanics (s-FCM).

This dissertation aims to develop structural models that account for scale effects to predict the mechanical response of structural elements over scales to a given external load. To achieve the stated objective, the s-FCM is relied upon. It assumes that using the fractional derivative allows the introduction of non-locality. It is because the fractional operators involve an interval whose size (in the approach used) relates to the length scale (microstructure grain size). Thus, it introduces the size of the interaction neighborhood of a specific material point.

The final results are space-Fractional Structural Mechanical Models (s-FSM), such as space-Fractional Beams and space-Fractional Plates. A numerical representation is created for each mathematical model developed, and a parametric study and validation are performed. The developed s-FSM models have only two additional parameters (order of fractional derivative and length scale) compared to their classical counterparts, and as both parameters control the scale effect in fractional models.

As mentioned, the new parameters of the s-FSM models relate to the material's microstructure. In particular, the length scale is set equal to the grain size. Consequently, a single set of parameters in statics and dynamics is obtained, which is unreachable in competitive non-local models. The results confirm that it is possible to return to classical models if the length scale's ratio to the structural element's external dimensions tends to zero or if the order of the fractional derivative is one. Most importantly, the s-FSM models are able to provide a good approximation of the experimental results for nano/micro-beams and nano/micro-plates.

Based on the results obtained, one can state that the aim of the dissertation has been achieved, and the thesis stated that *using the fractional derivative introduces the non-locality into structural mechanical models, allowing to capture scale effect* is correct.

# Streszczenie

Problem badawczy podjęty w rozprawie doktorskiej dotyczy modelowania elementów strukturalnych wykazujących efekt skali, np. elementów w skali nano i mikro. Zastosowanie klasycznej mechaniki ośrodków ciągłych jest nieodpowiednie w takim przypadku, ponieważ nie uwzględnia ona niejednorodności struktury materiałów (np. ziarnistej budowy, porowatości) co prowadzi do istotnych błędów modelowania przy dostatecznie małych skalach obserwacji. W małych skalach obserwacji występuje silny efekt skali oznaczający wpływ struktury wewnętrznej na zachowanie danego obiektu. Należy wówczas uwzględnić długość charakterystyczną struktury wewnętrznej (ang. *length scale*) w opisie zachowania rozpatrywanego ciała, szczególnie w skalach zbliżonych do wymiaru charakterystycznego mikrostruktury. Niezdolność klasycznej mechaniki ośrodków ciągłych do uwzględnienia efektu skali stanowiło motywację do opracowania uogólnionej (nielokalnej) teorii, tj. mechaniki ośrodków ciągłych niecałkowitego rzędu.

Celem niniejszej rozprawy doktorskiej jest opracowanie modeli strukturalnych uwzględniających efekt skali, aby umożliwić przewidywanie mechanicznej odpowiedzi elementów konstrukcyjnych w różnych skalach na zadane obciążenie zewnętrzne. Aby osiągnąć postawiony cel, wykorzystano założenia mechaniki ośrodków ciągłych niecałkowitego rzędu. Przyjmuje się, że zastosowanie pochodnej niecałkowitego rzędu pozwala na wprowadzenie nielokalności do modeli. Wynika to z faktu, iż pochodna niecałkowitego rzędu jest obliczana na pewnym przedziale, którego wielkość (w zastosowanym podejściu) związana jest z długością charakterystyczną struktury wewnętrznej. W ten sposób wprowadza się wielkość obszaru oddziaływania na dany punkt materialny.

Ostatecznym wynikiem rozprawy jest zdefiniowanie teorii strukturalnych, takich jak belki i płyty, w oparciu o mechanikę ośrodków ciągłych niecałkowitego rzędu. Dla każdego z modeli matematycznych stworzono reprezentację numeryczną oraz przeprowadzono studium parametryczne i walidację. Opracowane nielokalne modele strukturalne charakteryzują się ponadto tylko dwoma dodatkowymi parametrami odpowiedzialnymi za modelowanie efektu skali (rząd pochodnej i długość charakterystyczną struktury wewnętrznej) w porównaniu do ich klasycznych odpowiedników.

Jak wspomniano, nowe parametry zdefiniowanych modeli powiązane są z mikrostrukturą materiału - w szczególności długość charakterystyczna struktury wewnętrznej odpowiada wielkości ziarna. W związku z tym możliwe jest uzyskanie pojedynczego zestawu parametrów niezależnie czy rozważa się zagadnienie statyki czy dynamiki, co jest nieosiągalne w przypadku konkurencyjnych modeli nielokalnych. Uzyskane wyniki potwierdzają, że modele można zastąpić modelami klasycznymi, jeśli stosunek długości charakterystycznej struktury wewnętrznej do zewnętrznych wymiarów elementu konstrukcyjnego dąży do zera lub jeśli rząd pochodnej jest równy jeden. Najistotniejszym aspektem jest, że modele zapewniają dobre przybliżenie wyników eksperymentalnych dla nano/mikro belek i nano/mikro płyt.

Na podstawie uzyskanych wyników stwierdza się, że cel rozprawy doktorskiej został osiągnięty, a teza głosząca, że *wykorzystanie pochodnej niecałkowitego rzędu wprowadza nielokalność do strukturalnych modeli mechanicznych, pozwalając na opis efektu skali* jest poprawna.

# 1

# Introduction

## 1.1 Motivation

The classical continuum mechanics (CCM) deals with the macroscopic properties of material deformable bodies and assumes that material behavior is determined by local action independent of the change of the observation level scale [1]. However, most materials do not meet this assumption at the micro/nanoscale, as they demonstrate discontinuous (granular, porous) matter. CCM is therefore valid for macroscale bodies, whose geometric dimensions are much larger than those of the microstructure, and therefore each point of this medium represents a set of microscale elements (such for example, grains) with statistically homogeneous properties. At the same time, CCM fails in the description of micro- and nanoscale bodies, because the geometric dimensions of such a medium are too small to ignore the discontinuous (granular) structure of matter (see Fig. 1.1 - $\ell_f$ denotes the characteristic dimension of microstructure). Experimental observations indicate that mechanical properties are different at smaller (nano/micro) scales (see [2, 3, 4]). The scale effect here is the phenomenon involving the influence of the dimensions of a material body on its mechanical properties [5].

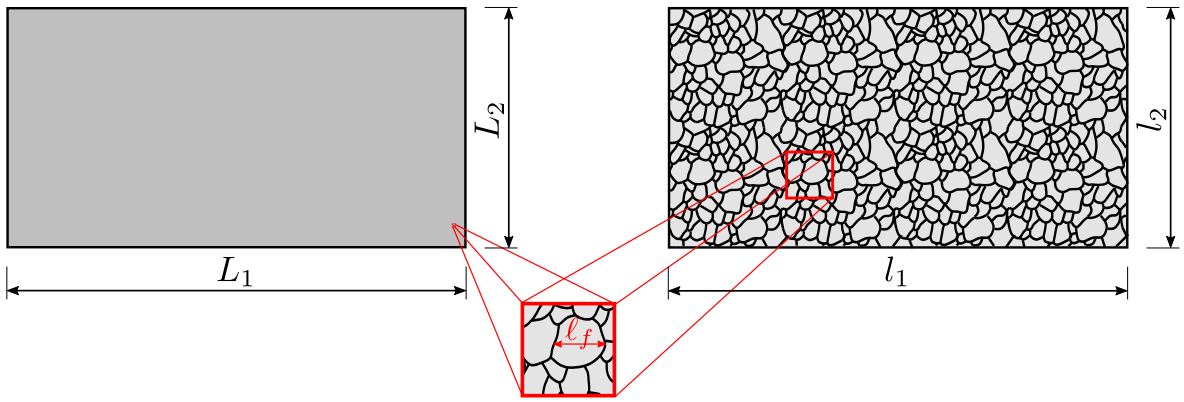


**Figure 1.1:** Macro-sized (on the left) and micro-sized body (on the right), where $\{L_1, L_2\} \gg \{l_1, l_2\}$ and $\{L_1, L_2\} \gg \ell_f$ (classical theory), and $\{l_1, l_2\} \sim \ell_f$ (non-local theory).

The still advancing miniaturization process brings the problem of scale effects to the main interest of modern science. Nano- and micro-electromechanical systems (NEMS/MEMS) are used in many daily-use devices (e.g., notebooks, smartphones) and industries: medical (hearing aids, blood pressure monitors), automotive (airbag sensors, parking sensors), aerospace (flight control systems, radars) [6]. The preparation of prototypes is time-consuming and economically unreasonable, so tools (mathematical models) for their efficient design (including design for load-bearing capacity and durability) are in great demand.

It is already known that CCM is unable to describe scale effects. Hence, there is a need for a general approach that accounts for material properties and structural behavior at different length scales [7, 8]. Concurrently, from an engineering point of view, methods that ensure the simplicity of continuum models while taking into account scale effects are desirable to satisfactorily and safely describe the behavior of such types of mediums. The scale effect, which is missing in CCM, must be added to the modeling strategy. This has been the motivation for the development of several generalized continuum models,

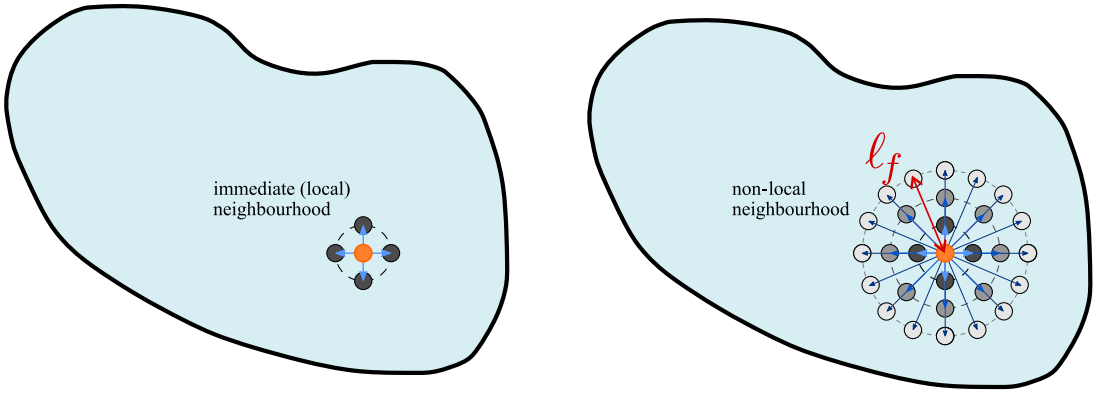


**Figure 1.2:** Neighborhood interaction of a material point in local and non-local theory.

called non-local theories (e.g. Eringen's integral theory [9], strain-gradient theory [10], stress-driven theory [11], peridynamics [12], micropolar theories [13]) - follow the reviews such as e.g. [14, 15, 8]. They contain scaling parameter that characterizes the internal structure of the material, also known in the literature as the *characteristic length* or *length scale*. Non-locality should be understood that the current answer of the model at the specific material point depends on the information from its finite neighborhood (the strain or intrinsic variable at a point is a weighted average of the values in a finite neighborhood). Compare that in the case of the CMM, the state of a material point is influenced by the material points in its immediate vicinity (Fig. 1.2). Non-local theories use a kind of homogenization to avoid the need for representing the complex original microstructure one-to-one. They generate an averaging of the internal structure under consideration so that the response of the model agrees with that of the complex one. Therefore, they are an effective tool for estimating the mechanical response of structures with scale effect, since being computationally less demanding than other methods, e.g. molecular dynamics. In consequence, the predictions produced by non-local models may be relevant for many industry sectors and useful in the design process.

Nonetheless, despite the existence of various non-local models attempting to describe scale effect, most of them lead to multiparametric models and may need different constitutive parameters depending on whether static or dynamic equilibrium is considered, or on the external (geometric) size of the analyzed nano/micro-body [16, 17, 18]. Therefore, appropriate methods of characterizing the scale effect are still being sought, and the need to improve existing models is still being recognized.

Considering the above brief explanation, the reader has perhaps already concluded that non-local theories are useful in analyzing elements whose geometric dimensions are of the nano- and micro-order. At this point, the author would like to point out that the applications of these theories are much more wide-reaching and are not limited to nano/micro-system problems but rather to the structures of heterogeneous and discontinuous nature. It can be said that the terms "nano" and "micro" here are figurative - the ratio of the body's geometric dimensions to the characteristic length of its internal structure is decisive. As in the case of micro-elements, the length scale can be related to the grain size, whereas in the case of other structures (even much larger than the micro order), it is related to the dimension of a certain repeatable and representative cell. Fig. 1.3 shows a few examples of structures for which non-local theories can be applied, including those found in civil engineering.

## 1.2 Research problem

Concluding the above introduction, the research subject undertaken is motivated by:

- The need to expand knowledge and understanding of scale effect.
- Inconsistencies between models of CCM and experimental results.
- Requiring different constitutive parameters in currently existing non-local models depending on whether one considers static or dynamic equilibrium, or on the external (geometric) size of the

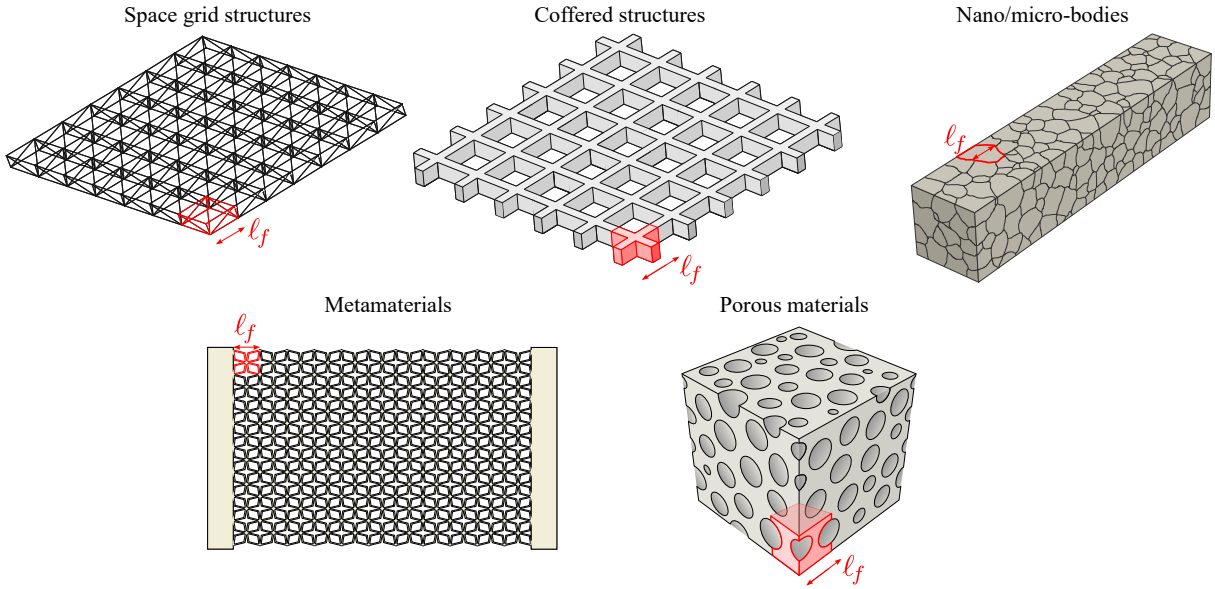


**Figure 1.3:** Example of structures with scale effect.

nano/micro-body, whereas they should be material parameters (constant for a specific microstructure).

- The need to develop appropriate mathematical and numerical models to analyze structures with scale effects.

Therefore, the main aim of the research is to develop structural models that take into account scale effects so that it will be possible to predict the mechanical response of structural elements over scales to a given external load. The research subjects are basic structural elements, namely beams and plates with scale effects. The models incorporating the scale effect are expected to meet the following requirements:

**R.1** Models have a limited number of new parameters.

**R.2** If the external characteristic length (structural element size) is much larger than the internal one (e.g. grain size), then the results of non-local continuum models align with the results of classical continuum models.

**R.3** New model parameters are associated with the microstructure of the material.

**R.4** The models represent real nano/micro-structural elements, so the results predicted by the models coincide with experimental findings.

The informativeness of the research is related to the method of accounting for non-locality. The scale effect is introduced by a fractional derivative (otherwise known as the derivative of non-integer order). Using the fractional calculus tool distinguishes the developed non-local models from competitively existing ones. To quote the statement of Harold T. Davis (1927) [19],

*"The great elegance that can be secured by the proper use of fractional operators and the power they have in simplifying the solution of complicated functional equations should more than justify a more general recognition and use."*

Based on the above, the following thesis for this dissertation is formulated:

**The use of the fractional derivative introduces the non-locality into structural mechanical models, allowing to capture the scale effect.**

## 1.3 Dissertation form

The dissertation consists of five original articles published in peer-reviewed scientific journals indexed in the Journal Citation Reports database:

**A.1** **P. Stempin** and W. Sumelka. *Space-fractional Euler-Bernoulli beam model - Theory and identification for silver nanobeam bending.* International Journal of Mechanical Sciences, 2020, 186, 105902. ($IF_{2020} = 5.329$)
DOI: 10.1016/j.ijmecsci.2020.105902

**A.2** **P. Stempin** and W. Sumelka. *Formulation and experimental validation of space-fractional Timoshenko beam model with functionally graded materials effects.* Computational Mechanics, 2021, 68, 697-708. ($IF_{2021} = 4.391$)
DOI: 10.1007/s00466-021-01987-6

**A.3** **P. Stempin** and W. Sumelka. *Dynamics of Space-Fractional Euler–Bernoulli and Timoshenko Beams.* Materials, 2021, 14, 1817. ($IF_{2021} = 3.748$)
DOI: 10.3390/ma14081817

**A.4** **P. Stempin** and W. Sumelka. *Space-fractional small-strain plasticity model for microbeams including grain size effect.* International Journal of Engineering Science, 2022, 175, 103672. ($IF_{2022} = 6.600$)
DOI: 10.1016/j.ijengsci.2022.103672

**A.5** **P. Stempin**, T. P. Pawlak and W. Sumelka. *Formulation of non-local space-fractional plate model and validation for composite micro-plates.* International Journal of Engineering Science, 2023, 192, 103932. ($IF_{2022} = 6.600$)
DOI: 10.1016/j.ijengsci.2023.103932

In Appendix A, the full texts of the publications are attached, while Appendix B contains the co-authors' statements. Although this document summarises the research presented in **Publications A.1÷A.5**, it can not be considered without them.

## 1.4 Outline

**Section 1: Introduction** This subsection closes the introduction and is preceded by a presentation of the motivation, research problem, and dissertation form.

**Section 2: Space-Fractional Structural Models**. This section covers the governing equations for the structural models in the framework of space-Fractional Continuum Mechanics. The research results involve the formulations of basic structural elements, such as space-fractional beams and space-fractional plates. Two beam models - space-Fractional Euler-Bernoulli Beam (s-FEBB) and space-Fractional Timoshenko Beam (s-FTB) were developed for statics (in elastic and elastic-plastic range) and dynamics, and two plate models - space-Fractional Kirchhoff-Love Plate (s-FKLP) and space-Fractional Mindlin-Reissner Plate (s-FMRP) for statics. Fig. 1.4 illustrates the scope of the research included in the dissertation, with reference to the publications that address the problem.

**Section 3: Parametric study and validation**. This section presents the results of the parametric study and validation. The parametric study presents how changes in new parameters affect the behavior of fractional structural models. The validation shows a comparison of the results predicted by fractional models and experimental data available in the literature for the nano/microbeams and nano/microplates.

**Section 4: Conclusions**. This section contains conclusions and future tasks.

**Bibliography** of this summary consists of 40 references, while

- **Publication A.1** - 65 references;

- **Publication A.2** - 46 references;
- **Publication A.3** - 49 references;
- **Publication A.4** - 67 references;
- **Publication A.5** - 74 references.

**Appendix A** contains the **Publications A.1÷A.5**.

All publications have a similar layout to this document, which covers sections on introduction, formulation of governing equations, numerical approximation, parametric study, validation, and conclusions.

**Appendix B** contains the co-authors' statements.

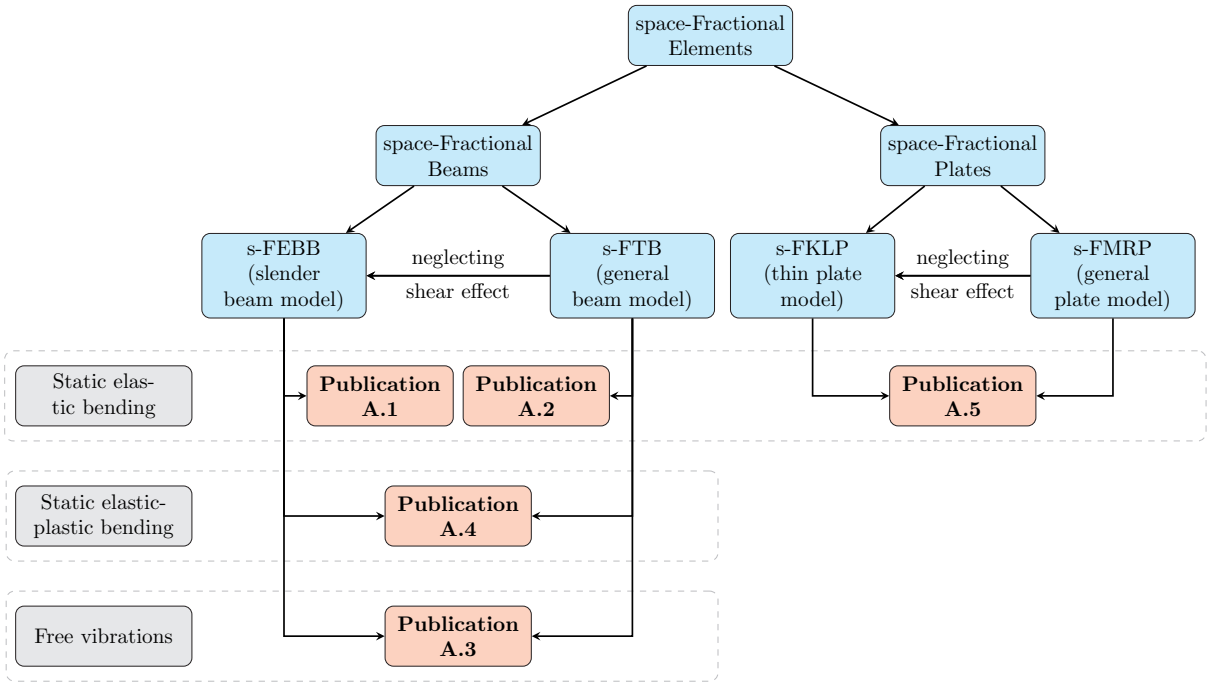


**Figure 1.4:** The scope of the research included in the dissertation, with reference to the publications that address the problem.

# 2

# Space-Fractional Structural Models

## 2.1 Selected aspects of fractional calculus

The author's goal is not to provide an in-depth explanation of fractional calculus, but a concise overview of its features utilized in the non-local theory being discussed, which are necessary for its accurate understanding. The reader interested in a more in-depth study of fractional calculus is referred to books, such as [20, 21].

The term fractional derivative means the derivative of arbitrary order. There are many definitions of fractional derivatives [22], however, the space-Fractional Continuum Mechanics (s-FCM) [23, 24] requires the fractional derivative of the constant to be zero, so standard boundary conditions are used as in classical differential equations. For this reason, the derivative of the Riesz-Caputo type is used,

$$ {}^{RC}_{x-\ell_f}D^{\alpha}_{x+\ell_f} f(x) = \frac{1}{2}\frac{\Gamma(2-\alpha)}{\Gamma(2)}\Big( {}^{C}_{x-\ell_f}D^{\alpha}_{x} f(x) + (-1)^n \, {}^{C}_{x}D^{\alpha}_{x+\ell_f} f(x)\Big), \tag{2.1} $$

which consists of the left-side and right-side Caputo derivatives

$$ {}^{C}_{x-\ell_f}D^{\alpha}_{x} f(x) = \frac{1}{\Gamma(n-\alpha)}\int_{x-\ell_f}^{x} \frac{f^{(n)}(\tau)}{(x-\tau)^{\alpha-n+1}}\mathrm{d}\tau, \tag{2.2} $$

$$ {}^{C}_{x}D^{\alpha}_{+\ell_f} f(x) = \frac{(-1)^n}{\Gamma(n-\alpha)}\int_{x}^{x+\ell_f} \frac{f^{(n)}(\tau)}{(\tau-x)^{\alpha-n+1}}\mathrm{d}\tau. \tag{2.3} $$

In the above, $\Gamma$ is an Euler gamma function, $n = \lfloor \alpha \rfloor + 1$, and $\lfloor . \rfloor$ denotes the integer part of a real number. Within the s-FCM, $\alpha$ is in the range $\alpha \in (0, 1]$. In addition, note that a fractional derivative here spans the distance $\ell_f$ to the left and right of the point $x$. In this way, the size of the neighborhood that interacts with the specific material point is inserted (cf. Fig. 1.2). Meanwhile, the kernel function (left $k^L_\alpha(x-\tau) = \frac{1}{(x-\tau)^{\alpha-n+1}}$ and right $k^R_\alpha(\tau-x) = \frac{1}{(\tau-x)^{\alpha-n+1}}$) weighs the contribution of the interacting neighborhood of the material point, where $\alpha$ determines its intensity.

The shortcut $\overset{\alpha}{\underset{x}{D}} f$ will appear throughout the rest of the thesis to stand for

$$ \overset{\alpha}{\underset{x}{D}} f = {}^{RC}_{x-\ell_f}D^{\alpha}_{x+\ell_f} f(x). \tag{2.4} $$

It is also clear that, for $\alpha = 1.0$, the classical first-order derivative is obtained

$$ \overset{1.0}{\underset{x}{D}} f = \frac{\mathrm{d}}{\mathrm{d}x} f. \tag{2.5} $$

## 2.2 Space-Fractional strains

In s-FCM, a definition of small Cauchy's strains is as follows [23, 24]

$$ \overset{\diamond}{\varepsilon}_{ij} = \frac{1}{2}\ell_f^{\alpha-1}\Big(\overset{\alpha}{\underset{x_j}{D}} u_i + \overset{\alpha}{\underset{x_i}{D}} u_j\Big), \tag{2.6} $$

where $\overset{\diamond}{\varepsilon}_{ij}$ is component of the fractional small strain tensor (see [25]), $u_i$, $u_j$ are components of the displacement vector. Likewise to Eq. (2.5), specifying $\alpha = 1.0$ results in a standard (local) definition of small Cauchy's strains

$$\varepsilon_{ij} = \frac{1}{2}\Big(\frac{\mathrm{d}}{\mathrm{d}x_j}u_i + \frac{\mathrm{d}}{\mathrm{d}x_i}u_j\Big). \tag{2.7}$$

The crucial parameters here are $\alpha$ and $\ell_f$, which arise due to using the fractional derivative Eq. (2.1). These parameters control the non-locality in the fractional elasticity and are additional material parameters to be identified for a specific material (see paper [26] which shows that the correspondence between microstructure topology and the fractional model is possible).

It should be added that the length scale is a certain function $\ell_f = \ell_f(\mathbf{x})$ that can reflect the distribution of the microstructure. The concept of variable length scale, as function decreasing at the boundaries [27], has been kept.

## 2.3 Space-Fractional Beams

The space-Fractional Beam is a structure that exhibits a scale effect and has one of its dimensions (length) much larger than the other two (see Fig. 2.1); e.g. nano/micro-beams, nano/micro-wires, nano/micro-rods or nano/micro-tubes. Two types of beam models were the subject of the study - the simpler s-FEBB theory, the scope of which is limited to slender beams due to the neglect of the effect of shear deformation on the rotation of the cross-section, and the s-FTB theory, which is a generalization of the s-FEBB theory. The developed space-fractional beam theories satisfy the following assumptions (with the first two assumptions identical to those in the classical approach [28]):

1. The cross-section of a beam is infinitely rigid in its own plane.
2. The cross-section of a beam remains a plane after deformation.
3. The cross-section of a beam rotates in proportion to the Riesz-Caputo fractional derivative with the proportionality factor $\ell_f^{\alpha-1}$ for s-FEBB, and it is extended by an additional rotation due to the fractional shear deformation $\overset{\diamond}{\gamma}_{13}$ for s-FTB, i.e.

$$\Phi_2 = \begin{cases} -\ell_f^{\alpha-1}\overset{\alpha}{\underset{x_1}{D}}\bar{u}_3 & \text{for s-FEBB,} \\ -\ell_f^{\alpha-1}\overset{\alpha}{\underset{x_1}{D}}\bar{u}_3 + \overset{\diamond}{\gamma}_{13} & \text{for s-FTB,} \end{cases} \tag{2.8}$$

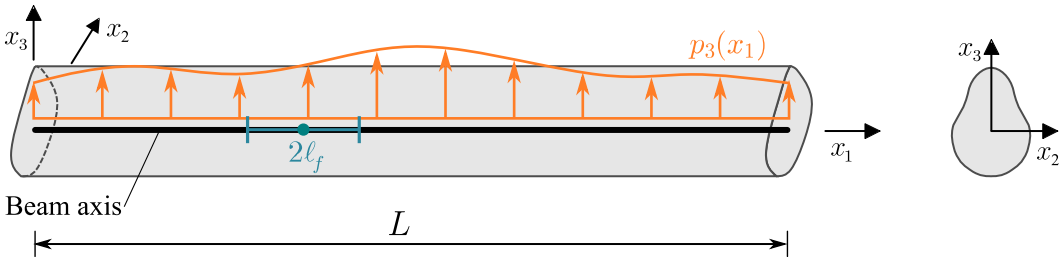


**Figure 2.1:** Schematic illustration of a beam and the coordinate system in the example of a beam of the length $L$ and an arbitrary cross-section. The length scale $\ell_f$ defines the surroundings that affect a given material point

Considerations are given to statics (elastic and elastic-plastic bending) and dynamics. In addition to the standard input data such as:

- beam geometry: length $L$; cross-section (moment of inertia $I$, area $A$, and the shear correction factor $k$);
- boundary conditions;
- distributed line load $p_3$;

- material parameters: elastic properties (Young's modulus $E$, Kirchhoff's modulus $G$), plastic properties (yield stress $\sigma_y$), and density $\rho$;

we need to provide the values of $\alpha$ and $\ell_f$, which are treated as parameters related to the microstructure. The final results, namely the governing equations (fractional differential equations) describing the behavior of space-fractional beams are listed below, while the complete derivation of the formulas is available in the publications.

- **Publication A.1** - s-FEBB theory for static elastic bending problem, for which the governing equation takes the form [29]

$$\overset{\alpha}{\underset{x_1}{D}}\left\{\ell_f^{\alpha-1}\overset{\alpha}{\underset{x_1}{D}}\left[\ell_f^{2\alpha-2}\overset{\alpha}{\underset{x_1}{D}}\left(\ell_f^{\alpha-1}\overset{\alpha}{\underset{x_1}{D}}\bar{u}_3\right)\right]\right\}EI = p_3. \tag{2.9}$$

  Eq. (2.9) describes the relationship between the beam deflection $\bar{u}_3$ and the applied distributed load $p_3$, assuming that the shear effect is negligible. It is appropriate for describing slender beams with scale effect.

- **Publication A.2** - s-FTB theory for static elastic bending problem, for which the governing equation takes the form [30]

$$\begin{cases} \overset{\alpha}{\underset{x_1}{D}}\left\{\ell_f^{\alpha-1}\overset{\alpha}{\underset{x_1}{D}}\left[\ell_f^{2\alpha-2}\overset{\alpha}{\underset{x_1}{D}}\left(\ell_f^{\alpha-1}\overset{\alpha}{\underset{x_1}{D}}\bar{u}_3\right)\right]\right\}EI = p_3 + \overset{\alpha}{\underset{x_1}{D}}\left[\ell_f^{\alpha-1}\overset{\alpha}{\underset{x_1}{D}}\left(\ell_f^{2\alpha-2}\overset{\alpha}{\underset{x_1}{D}}\overset{\diamond}{\gamma}_{13}\right)\right]EI, \\ \overset{\alpha}{\underset{x_1}{D}}\left[\ell_f^{2\alpha-2}\overset{\alpha}{\underset{x_1}{D}}\left(\ell_f^{\alpha-1}\overset{\alpha}{\underset{x_1}{D}}\bar{u}_3\right)\right]EI - \overset{\alpha}{\underset{x_1}{D}}\left(\ell_f^{2\alpha-2}\overset{\alpha}{\underset{x_1}{D}}\overset{\diamond}{\gamma}_{13}\right)EI + kGA\overset{\diamond}{\gamma}_{13} = 0; \end{cases} \tag{2.10}$$

  Eq. (2.10) describes the relationship between the beam deflection $\bar{u}_3$ and the applied distributed load $p_3$ without neglecting the shear effect ($\overset{\diamond}{\gamma}_{13}$). It is a more general model than s-FEBB and is not limited to describing slender beams with scale effect but also allows for thick ones.

- **Publication A.3** - s-FEBB and s-FTB theories for dynamics, for which the governing equations take the forms [31]

  – s-FEBB

$$\overset{\alpha}{\underset{x_1}{D}}\left\{\ell_f^{\alpha-1}\overset{\alpha}{\underset{x_1}{D}}\left[\ell_f^{2\alpha-2}\overset{\alpha}{\underset{x_1}{D}}\left(\ell_f^{\alpha-1}\overset{\alpha}{\underset{x_1}{D}}\bar{u}_3(t)\right)\right]\right\}EI + \rho A\ddot{\bar{u}}_3(t) = p_3(t) \tag{2.11}$$

  – s-FTB

$$\begin{cases} \overset{\alpha}{\underset{x_1}{D}}\left\{\ell_f^{\alpha-1}\overset{\alpha}{\underset{x_1}{D}}\left[\ell_f^{2\alpha-2}\overset{\alpha}{\underset{x_1}{D}}\left(\ell_f^{\alpha-1}\overset{\alpha}{\underset{x_1}{D}}\bar{u}_3\right)\right]\right\}EI - \overset{\alpha}{\underset{x_1}{D}}\left[\ell_f^{\alpha-1}\overset{\alpha}{\underset{x_1}{D}}\left(\ell_f^{2\alpha-2}\overset{\alpha}{\underset{x_1}{D}}\overset{\diamond}{\gamma}_{13}\right)\right]EI + \\ \quad - \rho I\overset{\alpha}{\underset{x_1}{D}}\left(\ell_f^{2\alpha-2}\overset{\alpha}{\underset{x_1}{D}}\ddot{\bar{u}}_3\right) + \rho A\ddot{\bar{u}}_3 + \rho I\overset{\alpha}{\underset{x_1}{D}}\left(\ell_f^{\alpha-1}\ddot{\overset{\diamond}{\gamma}}_{13}\right) = p_3; \\ \overset{\alpha}{\underset{x_1}{D}}\left\{\ell_f^{2\alpha-2}\left[\overset{\alpha}{\underset{x_1}{D}}\left(\ell_f^{\alpha-1}\overset{\alpha}{\underset{x_1}{D}}\bar{u}_3\right) - \overset{\alpha}{\underset{x_1}{D}}\overset{\diamond}{\gamma}_{13}\right]\right\}EI - \rho I\left(\ell_f^{\alpha-1}\overset{\alpha}{\underset{x_1}{D}}\ddot{\bar{u}}_3 - \ddot{\overset{\diamond}{\gamma}}_{13}\right) + kGA\overset{\diamond}{\gamma}_{13} = 0. \end{cases} \tag{2.12}$$

  Eq. (2.11) and Eq. (2.12) describe the relationship between the beam deflection $\bar{u}_3(t)$ and the applied distributed load $p_3(t)$ at time $t$, assuming that the shear effect is neglected/included, respectively. Symbol $\ddot{(.)}$ denotes the second derivative with respect to time.

  In the case of free vibrations, the governing equation takes the form for the s-FEBB model:

$$\overset{\alpha}{\underset{x_1}{D}}\left\{\ell_f^{\alpha-1}\overset{\alpha}{\underset{x_1}{D}}\left[\ell_f^{2\alpha-2}\overset{\alpha}{\underset{x_1}{D}}\left(\ell_f^{\alpha-1}\overset{\alpha}{\underset{x_1}{D}}\bar{u}_3\right)\right]\right\}EI - \rho A\omega^2\bar{u}_3 = 0; \tag{2.13}$$

  and for the s-FTB model:

$$\begin{cases} \overset{\alpha}{\underset{x_1}{D}}\left\{\ell_f^{\alpha-1}\overset{\alpha}{\underset{x_1}{D}}\left[\ell_f^{2\alpha-2}\overset{\alpha}{\underset{x_1}{D}}\left(\ell_f^{\alpha-1}\overset{\alpha}{\underset{x_1}{D}}\bar{u}_3\right)\right]\right\}EI - \overset{\alpha}{\underset{x_1}{D}}\left[\ell_f^{\alpha-1}\overset{\alpha}{\underset{x_1}{D}}\left(\ell_f^{2\alpha-2}\overset{\alpha}{\underset{x_1}{D}}\overset{\diamond}{\gamma}_{13}\right)\right]EI \\ \quad + \rho I\omega^2\overset{\alpha}{\underset{x_1}{D}}\left(\ell_f^{2\alpha-2}\overset{\alpha}{\underset{x_1}{D}}\bar{u}_3\right) - \rho A\omega^2\bar{u}_3 - \rho I\omega^2\overset{\alpha}{\underset{x_1}{D}}\left(\ell_f^{\alpha-1}\overset{\diamond}{\gamma}_{13}\right) = 0; \\ \overset{\alpha}{\underset{x_1}{D}}\left\{\ell_f^{2\alpha-2}\left[\overset{\alpha}{\underset{x_1}{D}}\left(\ell_f^{\alpha-1}\overset{\alpha}{\underset{x_1}{D}}\bar{u}_3\right) - \overset{\alpha}{\underset{x_1}{D}}\overset{\diamond}{\gamma}_{13}\right]\right\}EI + kGA\overset{\diamond}{\gamma} + \rho I\omega^2\left(\ell_f^{\alpha-1}\overset{\alpha}{\underset{x_1}{D}}\bar{u}_3 - \overset{\diamond}{\gamma}_{13}\right) = 0. \end{cases} \tag{2.14}$$

  Solving the eigenproblem allows to get the eigenvectors $\bar{u}_3$ (shape of modes) and the circular frequencies $\omega$.

- **Publication A.4** - s-FEBB and s-FTB theories for static elastic-plastic bending problem, for which the governing equation takes the form [32]

  – s-FEBB

$$-\overset{\alpha}{\underset{x_1}{D}}\Big[\ell_f^{\alpha-1}\overset{\alpha}{\underset{x_1}{D}}\Big(\ell_f^{\alpha-1}\int_A x_3(\overset{\diamond}{\varepsilon}_{11}-\gamma N_{11})\,\mathrm{d}A\Big)\Big]E=p_3 \tag{2.15}$$

  – s-FTB

$$\begin{cases}-\overset{\alpha}{\underset{x_1}{D}}\Big[\ell_f^{\alpha-1}\overset{\alpha}{\underset{x_1}{D}}\Big(\ell_f^{\alpha-1}\int_A x_3(\overset{\diamond}{\varepsilon}_{11}-\gamma N_{11})\,\mathrm{d}A\Big)\Big]E=p_3\\ \overset{\alpha}{\underset{x_1}{D}}\Big(\ell_f^{\alpha-1}\int_A x_3(\overset{\diamond}{\varepsilon}_{11}-\gamma N_{11})E\,\mathrm{d}A\Big)=kG\int_A(\overset{\diamond}{\gamma}_{13}-\gamma N_{13})\,\mathrm{d}A\end{cases} \tag{2.16}$$

  where $\gamma$ is plastic multiplier, and $N_{11}$ and $N_{13}$ are components of plastic flow vector $\mathbf{N}=\frac{\partial f}{\partial\sigma}$. The yield function $f(\boldsymbol{\sigma},\sigma_y)$ depends on the current stress state $\boldsymbol{\sigma}$ and the yield stress $\sigma_y$,

$$\begin{cases}f(\boldsymbol{\sigma},\sigma_y)<0 & \text{for elastic region,}\\ f(\boldsymbol{\sigma},\sigma_y)=0 & \text{for plastic region,}\end{cases} \tag{2.17}$$

  where the yield function $f(\boldsymbol{\sigma},\sigma_y)$ is expressed as

$$f(\boldsymbol{\sigma},\sigma_y)=\sigma_v-\sigma_y\ . \tag{2.18}$$

  Equivalent stress $\sigma_v$ depends on the assumed criterion of plasticity.

In all cases setting $\alpha\to 1.0$ or $\ell_f\to 0$ reproduces CCM beam models [33], for example, Eq. (2.9) for the s-FEBB model takes the form

$$\frac{\mathrm{d}^4\bar{u}_3}{\mathrm{d}x_1^4}EI=p_3. \tag{2.19}$$

## 2.4 Space-Fractional Plates

The space-Fractional Plate is a structure that exhibits a scale effect and has one of its dimensions (thickness) much smaller than the other two (see Fig. 2.2); e.g. nano/micro-structures, such as nano/micro-plates, thin films, or nano/micro-sheets. Two types of fractional plate models were the subject of the study - the simpler s-FKLP theory, the scope of which is limited to thin plates due to the neglect of the effect of shear deformation on the rotations of normal to the middle plane, and the s-FMRP theory, which is a generalization of the s-FKLP theory. The developed space-fractional plate theories satisfy the following assumptions (with the first two being identical to those known from the classical approach [28]):

1. The normal material line is infinitely rigid along its own length.
2. The normal material line of the plate remains a straight line after deformation.
3. The straight normal material line rotates in proportion to the Riesz-Caputo fractional derivative with the proportionality factor $\ell_f^{\alpha-1}$ for s-FKLP, and it is extended by additional rotations due to the fractional shear deformations ($\overset{\diamond}{\gamma}_{13}$ and $\overset{\diamond}{\gamma}_{23}$) for s-FMRP, i.e.

$$\Phi_1=\begin{cases}\ell_f^{\alpha-1}\overset{\alpha}{\underset{x_2}{D}}\bar{u}_3 & \text{for s-FKLP,}\\ \ell_f^{\alpha-1}\overset{\alpha}{\underset{x_2}{D}}\bar{u}_3-\overset{\diamond}{\gamma}_{23} & \text{for s-FMRP,}\end{cases}\qquad \Phi_2=\begin{cases}-\ell_f^{\alpha-1}\overset{\alpha}{\underset{x_1}{D}}\bar{u}_3 & \text{for s-FKLP,}\\ -\ell_f^{\alpha-1}\overset{\alpha}{\underset{x_1}{D}}\bar{u}_3+\overset{\diamond}{\gamma}_{13} & \text{for s-FMRP.}\end{cases} \tag{2.20}$$

Considerations are given to statics (elastic bending). As with space-fractional beams, in addition to the standard input data such as:

- plate geometry: length $L_{x_1}$ and width $L_{x_2}$ (for rectangular plate), thickness $t$, shear correction factor $k$;
- boundary conditions;
- distributed surface load $p_3$;

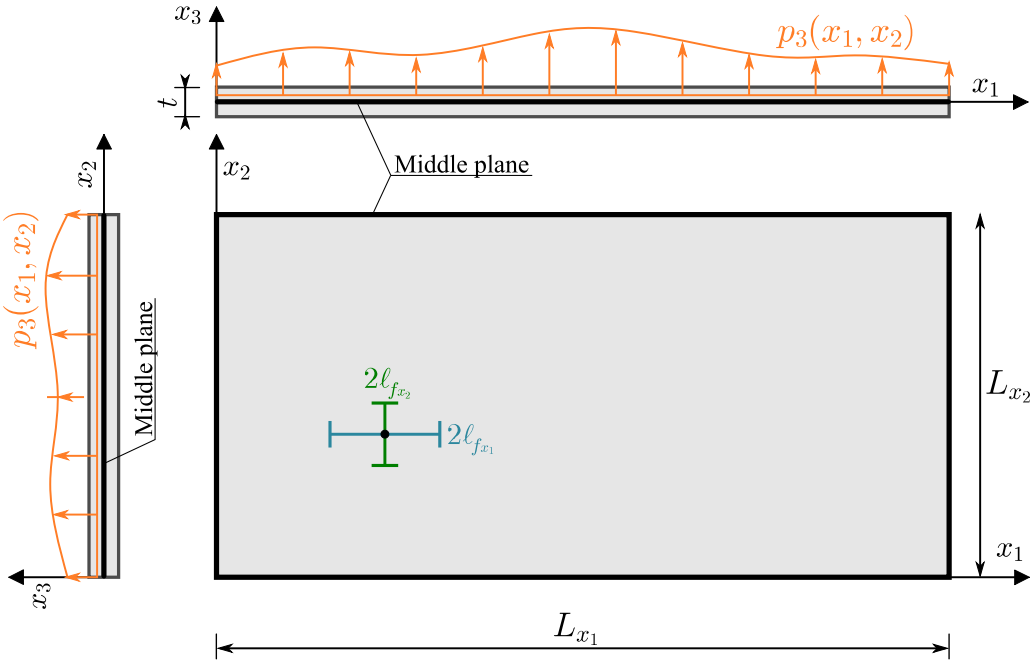


**Figure 2.2:** Schematic illustration of a plate and the coordinate system in the example of a rectangular plate of thickness $t$ and dimensions in the plane $L_{x_1}$ and $L_{x_1}$, loaded with a mechanical transverse distributed load $p_3(x_1, x_2)$ on the plate surface. The length scales $\ell_{f_{x_1}}$ and $\ell_{f_{x_1}}$ define the surroundings that affect a given material point in the $x_1$ and $x_2$ directions, respectively.

- material parameters: elastic properties (Young's modulus $E$, Poisson's ration $\nu$, Kirchhoff's modulus $G = \frac{E}{2(1+\nu)}$);

we need to provide the values of $\alpha$ and $\ell_f$, which are treated as parameters related to the microstructure. The final results, namely the governing equations (fractional partial differential equations) describing the behavior of space-fractional plates are listed below, while the complete derivation of the formulas is available in the publications:

- **Publication A.5** - s-FKLP theory for static elastic bending problem, for which the governing equation takes the form [34]

$$\begin{aligned}
&\mathsf{D}^{m_2}\overset{\alpha}{D}_{x_1}\Big\{\ell_{f_{x_1}}^{\alpha-1}\overset{\alpha}{D}_{x_1}\Big[\ell_{f_{x_1}}^{2\alpha-2}\overset{\alpha}{D}_{x_1}\Big(\ell_{f_{x_1}}^{\alpha-1}\overset{\alpha}{D}_{x_1}\bar{u}_3\Big)\Big]\Big\} + \mathsf{D}^{m_1}\overset{\alpha}{D}_{x_1}\Big\{\ell_{f_{x_1}}^{\alpha-1}\overset{\alpha}{D}_{x_1}\Big[\ell_{f_{x_1}}^{\alpha-1}\ell_{f_{x_2}}^{\alpha-1}\overset{\alpha}{D}_{x_2}\Big(\ell_{f_{x_2}}^{\alpha-1}\overset{\alpha}{D}_{x_2}\bar{u}_3\Big)\Big]\Big\}+\\
&\mathsf{D}^{m_3}\overset{\alpha}{D}_{x_1}\Big\{\ell_{f_{x_1}}^{\alpha-1}\overset{\alpha}{D}_{x_2}\Big[\ell_{f_{x_2}}^{2\alpha-2}\overset{\alpha}{D}_{x_2}\Big(\ell_{f_{x_1}}^{\alpha-1}\overset{\alpha}{D}_{x_1}\bar{u}_3\Big)\Big]\Big\} + \mathsf{D}^{m_3}\overset{\alpha}{D}_{x_1}\Big\{\ell_{f_{x_1}}^{\alpha-1}\overset{\alpha}{D}_{x_2}\Big[\ell_{f_{x_2}}^{\alpha-1}\ell_{f_{x_1}}^{\alpha-1}\overset{\alpha}{D}_{x_1}\Big(\ell_{f_{x_2}}^{\alpha-1}\overset{\alpha}{D}_{x_2}\bar{u}_3\Big)\Big]\Big\}+\\
&\mathsf{D}^{m_1}\overset{\alpha}{D}_{x_2}\Big\{\ell_{f_{x_2}}^{\alpha-1}\overset{\alpha}{D}_{x_2}\Big[\ell_{f_{x_2}}^{\alpha-1}\ell_{f_{x_1}}^{\alpha-1}\overset{\alpha}{D}_{x_1}\Big(\ell_{f_{x_1}}^{\alpha-1}\overset{\alpha}{D}_{x_1}\bar{u}_3\Big)\Big]\Big\} + \mathsf{D}^{m_2}\overset{\alpha}{D}_{x_2}\Big\{\ell_{f_{x_2}}^{\alpha-1}\overset{\alpha}{D}_{x_2}\Big[\ell_{f_{x_2}}^{2\alpha-2}\overset{\alpha}{D}_{x_2}\Big(\ell_{f_{x_2}}^{\alpha-1}\overset{\alpha}{D}_{x_2}\bar{u}_3\Big)\Big]\Big\}+\\
&\mathsf{D}^{m_3}\overset{\alpha}{D}_{x_2}\Big\{\ell_{f_{x_2}}^{\alpha-1}\overset{\alpha}{D}_{x_1}\Big[\ell_{f_{x_1}}^{\alpha-1}\ell_{f_{x_2}}^{\alpha-1}\overset{\alpha}{D}_{x_2}\Big(\ell_{f_{x_1}}^{\alpha-1}\overset{\alpha}{D}_{x_1}\bar{u}_3\Big)\Big]\Big\} + \mathsf{D}^{m_3}\overset{\alpha}{D}_{x_2}\Big\{\ell_{f_{x_2}}^{\alpha-1}\overset{\alpha}{D}_{x_1}\Big[\ell_{f_{x_1}}^{2\alpha-2}\overset{\alpha}{D}_{x_1}\Big(\ell_{f_{x_2}}^{\alpha-1}\overset{\alpha}{D}_{x_2}\bar{u}_3\Big)\Big]\Big\} = p_3
\end{aligned} \tag{2.21}$$

where cross-sectional stiffnesses $D^{m_1}$, $D^{m_2}$ and $D^{m_3}$ are defined as

$$\begin{Bmatrix}\mathsf{D}^{m_1}\\ \mathsf{D}^{m_2}\\ \mathsf{D}^{m_3}\end{Bmatrix} = \begin{Bmatrix}\int_t x_3^2 \frac{\nu E}{1-\nu^2}\mathrm{d}x_3\\ \int_t x_3^2 \frac{E}{1-\nu^2}\mathrm{d}x_3\\ \int_t x_3^2 G\mathrm{d}x_3\end{Bmatrix}. \tag{2.22}$$

Eq. (2.21) describes the relationship between the plate deflection $\bar{u}_3$ and the applied distributed load $p_3$, assuming that the shear effect is negligible. It is appropriate for describing thin plates with scale effect.

- s-FMRP theory (by analogy to s-FKLP) for static elastic bending problem (results unpublished yet), for which the governing equation takes the form

$$
\begin{cases}
\mathsf{D}^{m_2}\overset{\alpha}{D}_{x_1}\Big\{\ell_{f_{x_1}}^{\alpha-1}\overset{\alpha}{D}_{x_1}\Big[\ell_{f_{x_1}}^{2\alpha-2}\overset{\alpha}{D}_{x_1}\Big(\ell_{f_{x_1}}^{\alpha-1}\overset{\alpha}{D}_{x_1}\bar{u}_3\Big)\Big]\Big\}+\mathsf{D}^{m_1}\overset{\alpha}{D}_{x_1}\Big\{\ell_{f_{x_1}}^{\alpha-1}\overset{\alpha}{D}_{x_1}\Big[\ell_{f_{x_1}}^{\alpha-1}\ell_{f_{x_2}}^{\alpha-1}\overset{\alpha}{D}_{x_2}\Big(\ell_{f_{x_2}}^{\alpha-1}\overset{\alpha}{D}_{x_2}\bar{u}_3\Big)\Big]\Big\}\\
\quad+\mathsf{D}^{m_3}\overset{\alpha}{D}_{x_1}\Big\{\ell_{f_{x_1}}^{\alpha-1}\overset{\alpha}{D}_{x_2}\Big[\ell_{f_{x_2}}^{2\alpha-2}\overset{\alpha}{D}_{x_2}\Big(\ell_{f_{x_1}}^{\alpha-1}\overset{\alpha}{D}_{x_1}\bar{u}_3\Big)\Big]\Big\}+\mathsf{D}^{m_3}\overset{\alpha}{D}_{x_1}\Big\{\ell_{f_{x_1}}^{\alpha-1}\overset{\alpha}{D}_{x_2}\Big[\ell_{f_{x_2}}^{\alpha-1}\ell_{f_{x_1}}^{\alpha-1}\overset{\alpha}{D}_{x_1}\Big(\ell_{f_{x_2}}^{\alpha-1}\overset{\alpha}{D}_{x_2}\bar{u}_3\Big)\Big]\Big\}\\
\quad+\mathsf{D}^{m_1}\overset{\alpha}{D}_{x_2}\Big\{\ell_{f_{x_2}}^{\alpha-1}\overset{\alpha}{D}_{x_2}\Big[\ell_{f_{x_2}}^{\alpha-1}\ell_{f_{x_1}}^{\alpha-1}\overset{\alpha}{D}_{x_1}\Big(\ell_{f_{x_1}}^{\alpha-1}\overset{\alpha}{D}_{x_1}\bar{u}_3\Big)\Big]\Big\}+\mathsf{D}^{m_2}\overset{\alpha}{D}_{x_2}\Big\{\ell_{f_{x_2}}^{\alpha-1}\overset{\alpha}{D}_{x_2}\Big[\ell_{f_{x_2}}^{2\alpha-2}\overset{\alpha}{D}_{x_2}\Big(\ell_{f_{x_2}}^{\alpha-1}\overset{\alpha}{D}_{x_2}\bar{u}_3\Big)\Big]\Big\}\\
\quad+\mathsf{D}^{m_3}\overset{\alpha}{D}_{x_2}\Big\{\ell_{f_{x_2}}^{\alpha-1}\overset{\alpha}{D}_{x_1}\Big[\ell_{f_{x_1}}^{\alpha-1}\ell_{f_{x_2}}^{\alpha-1}\overset{\alpha}{D}_{x_2}\Big(\ell_{f_{x_1}}^{\alpha-1}\overset{\alpha}{D}_{x_1}\bar{u}_3\Big)\Big]\Big\}+\mathsf{D}^{m_3}\overset{\alpha}{D}_{x_2}\Big\{\ell_{f_{x_2}}^{\alpha-1}\overset{\alpha}{D}_{x_1}\Big[\ell_{f_{x_1}}^{2\alpha-2}\overset{\alpha}{D}_{x_1}\Big(\ell_{f_{x_2}}^{\alpha-1}\overset{\alpha}{D}_{x_2}\bar{u}_3\Big)\Big]\Big\}\\
\quad-\mathsf{D}^{m_2}\overset{\alpha}{D}_{x_1}\Big\{\ell_{f_{x_1}}^{\alpha-1}\overset{\alpha}{D}_{x_1}\Big[\ell_{f_{x_1}}^{2\alpha-2}\overset{\alpha}{D}_{x_1}\overset{\diamond}{\gamma}_{13}\Big]\Big\}-\mathsf{D}^{m_3}\overset{\alpha}{D}_{x_1}\Big\{\ell_{f_{x_1}}^{\alpha-1}\overset{\alpha}{D}_{x_2}\Big[\ell_{f_{x_2}}^{2\alpha-2}\overset{\alpha}{D}_{x_2}\overset{\diamond}{\gamma}_{13}\Big]\Big\}\\
\quad-\mathsf{D}^{m_1}\overset{\alpha}{D}_{x_2}\Big\{\ell_{f_{x_2}}^{\alpha-1}\overset{\alpha}{D}_{x_2}\Big[\ell_{f_{x_2}}^{\alpha-1}\ell_{f_{x_1}}^{\alpha-1}\overset{\alpha}{D}_{x_1}\overset{\diamond}{\gamma}_{13}\Big]\Big\}-\mathsf{D}^{m_3}\overset{\alpha}{D}_{x_2}\Big\{\ell_{f_{x_2}}^{\alpha-1}\overset{\alpha}{D}_{x_1}\Big[\ell_{f_{x_1}}^{\alpha-1}\ell_{f_{x_2}}^{\alpha-1}\overset{\alpha}{D}_{x_2}\overset{\diamond}{\gamma}_{13}\Big]\Big\}\\
\quad-\mathsf{D}^{m_1}\overset{\alpha}{D}_{x_1}\Big\{\ell_{f_{x_1}}^{\alpha-1}\overset{\alpha}{D}_{x_1}\Big[\ell_{f_{x_1}}^{\alpha-1}\ell_{f_{x_2}}^{\alpha-1}\overset{\alpha}{D}_{x_2}\overset{\diamond}{\gamma}_{23}\Big]\Big\}-\mathsf{D}^{m_3}\overset{\alpha}{D}_{x_1}\Big\{\ell_{f_{x_1}}^{\alpha-1}\overset{\alpha}{D}_{x_2}\Big[\ell_{f_{x_2}}^{\alpha-1}\ell_{f_{x_1}}^{\alpha-1}\overset{\alpha}{D}_{x_1}\overset{\diamond}{\gamma}_{23}\Big]\Big\}+\\
\quad-\mathsf{D}^{m_2}\overset{\alpha}{D}_{x_2}\Big\{\ell_{f_{x_2}}^{\alpha-1}\overset{\alpha}{D}_{x_2}\Big[\ell_{f_{x_2}}^{2\alpha-2}\overset{\alpha}{D}_{x_2}\overset{\diamond}{\gamma}_{23}\Big]\Big\}-\mathsf{D}^{m_3}\overset{\alpha}{D}_{x_2}\Big\{\ell_{f_{x_2}}^{\alpha-1}\overset{\alpha}{D}_{x_1}\Big[\ell_{f_{x_1}}^{2\alpha-2}\overset{\alpha}{D}_{x_1}\overset{\diamond}{\gamma}_{23}\Big]\Big\}=p_3;\\
-\Big\{\mathsf{D}^{m_2}\overset{\alpha}{D}_{x_1}\Big[\ell_{f_{x_1}}^{2\alpha-2}\overset{\alpha}{D}_{x_1}\Big(\ell_{f_{x_1}}^{\alpha-1}\overset{\alpha}{D}_{x_1}\bar{u}_3\Big)\Big]+\mathsf{D}^{m_1}\overset{\alpha}{D}_{x_1}\Big[\ell_{f_{x_1}}^{\alpha-1}\ell_{f_{x_2}}^{\alpha-1}\overset{\alpha}{D}_{x_2}\Big(\ell_{f_{x_2}}^{\alpha-1}\overset{\alpha}{D}_{x_2}\bar{u}_3\Big)\Big]+\\
\quad+\mathsf{D}^{m_3}\overset{\alpha}{D}_{x_2}\Big[\ell_{f_{x_2}}^{2\alpha-2}\overset{\alpha}{D}_{x_2}\Big(\ell_{f_{x_1}}^{\alpha-1}\overset{\alpha}{D}_{x_1}\bar{u}_3\Big)\Big]+\mathsf{D}^{m_3}\overset{\alpha}{D}_{x_2}\Big[\ell_{f_{x_2}}^{\alpha-1}\ell_{f_{x_1}}^{\alpha-1}\overset{\alpha}{D}_{x_1}\Big(\ell_{f_{x_2}}^{\alpha-1}\overset{\alpha}{D}_{x_2}\bar{u}_3\Big)\Big]\Big\}\\
\quad+\Big\{\mathsf{D}^{m_2}\overset{\alpha}{D}_{x_1}\Big[\ell_{f_{x_1}}^{2\alpha-2}\overset{\alpha}{D}_{x_1}\overset{\diamond}{\gamma}_{13}\Big]+\mathsf{D}^{m_3}\overset{\alpha}{D}_{x_2}\Big[\ell_{f_{x_2}}^{2\alpha-2}\overset{\alpha}{D}_{x_2}\overset{\diamond}{\gamma}_{13}\Big]-\mathsf{D}^{m_4}\overset{\diamond}{\gamma}_{13}\Big\}\\
\quad+\Big\{\mathsf{D}^{m_1}\overset{\alpha}{D}_{x_1}\Big[\ell_{f_{x_1}}^{\alpha-1}\ell_{f_{x_2}}^{\alpha-1}\overset{\alpha}{D}_{x_2}\overset{\diamond}{\gamma}_{23}\Big]+\mathsf{D}^{m_3}\overset{\alpha}{D}_{x_2}\Big[\ell_{f_{x_2}}^{\alpha-1}\ell_{f_{x_1}}^{\alpha-1}\overset{\alpha}{D}_{x_1}\overset{\diamond}{\gamma}_{23}\Big]\Big\}=0;\\
-\Big\{\mathsf{D}^{m_1}\overset{\alpha}{D}_{x_2}\Big[\ell_{f_{x_2}}^{\alpha-1}\ell_{f_{x_1}}^{\alpha-1}\overset{\alpha}{D}_{x_1}\Big(\ell_{f_{x_1}}^{\alpha-1}\overset{\alpha}{D}_{x_1}\bar{u}_3\Big)\Big]+\mathsf{D}^{m_2}\overset{\alpha}{D}_{x_2}\Big[\ell_{f_{x_2}}^{2\alpha-2}\overset{\alpha}{D}_{x_2}\Big(\ell_{f_{x_2}}^{\alpha-1}\overset{\alpha}{D}_{x_2}\bar{u}_3\Big)\Big]\\
\quad+\mathsf{D}^{m_3}\overset{\alpha}{D}_{x_1}\Big[\ell_{f_{x_1}}^{\alpha-1}\ell_{f_{x_2}}^{\alpha-1}\overset{\alpha}{D}_{x_2}\Big(\ell_{f_{x_1}}^{\alpha-1}\overset{\alpha}{D}_{x_1}\bar{u}_3\Big)\Big]+\mathsf{D}^{m_3}\overset{\alpha}{D}_{x_1}\Big[\ell_{f_{x_1}}^{2\alpha-2}\overset{\alpha}{D}_{x_1}\Big(\ell_{f_{x_2}}^{\alpha-1}\overset{\alpha}{D}_{x_2}\bar{u}_3\Big)\Big]\Big\}\\
\quad+\Big\{\mathsf{D}^{m_1}\overset{\alpha}{D}_{x_2}\Big[\ell_{f_{x_2}}^{\alpha-1}\ell_{f_{x_1}}^{\alpha-1}\overset{\alpha}{D}_{x_1}\overset{\diamond}{\gamma}_{13}\Big]+\mathsf{D}^{m_3}\overset{\alpha}{D}_{x_1}\Big[\ell_{f_{x_1}}^{\alpha-1}\ell_{f_{x_2}}^{\alpha-1}\overset{\alpha}{D}_{x_2}\overset{\diamond}{\gamma}_{13}\Big]\Big\}\\
\quad+\Big\{\mathsf{D}^{m_2}\overset{\alpha}{D}_{x_2}\Big[\ell_{f_{x_2}}^{2\alpha-2}\overset{\alpha}{D}_{x_2}\overset{\diamond}{\gamma}_{23}\Big]+\mathsf{D}^{m_3}\overset{\alpha}{D}_{x_1}\Big[\ell_{f_{x_1}}^{2\alpha-2}\overset{\alpha}{D}_{x_1}\overset{\diamond}{\gamma}_{23}\Big]-\mathsf{D}^{m_4}\overset{\diamond}{\gamma}_{13}\Big\}=0;
\end{cases}
\tag{2.23}
$$

where

$$
\mathsf{D}^{m_4}=\int_t kG\,\mathrm{d}x_3. \tag{2.24}
$$

Eq. (2.23) describes the relationship between the plate deflection $\bar{u}_3$ and the applied distributed load $p_3$ without neglecting the shear effect. It is a more general model than s-FKLP and is not limited to describing thin plates with scale effect but also allows for thick ones.

In all cases setting $\alpha \to 1.0$ or $\ell_f \to 0$ reproduces CCM plate models [33], for example, Eq. (2.21) for the s-FKLP model takes the form

$$
\mathsf{D}\Big(\frac{\mathrm{d}^4\bar{u}_3}{\mathrm{d}x_1^4}+2\frac{\mathrm{d}^4\bar{u}_3}{\mathrm{d}x_1^2\mathrm{d}x_2^2}+\frac{\mathrm{d}^4\bar{u}_3}{\mathrm{d}x_2^4}\Big)=p_3, \tag{2.25}
$$

where cross-sectional stiffness is

$$
\mathsf{D}=\int_t x_3^2\frac{E}{1-\nu^2}\mathrm{d}x_3=\frac{Et^3}{12(1-\nu^2)}. \tag{2.26}
$$

# 3

# Parametric study and validation

## 3.1 Numerical approximation

For each governing equation Eq. (2.9)÷(2.23) presented in Section 2, an original numerical representation was developed based on approximating the fractional derivative Eq. (2.1) with a trapezoidal rule [35, 21],

$$\overset{\alpha}{\underset{x}{D}}( \ . \ )_i = \Delta x^{1-\alpha} \mathsf{A} \Big[ \mathsf{B}( \ . \ )'_{i-m} + \sum_{j^a=i-m+1}^{i-1} \mathsf{C}^a( \ . \ )'_{j^a} + 2( \ . \ )'_i + \sum_{j^b=i+1}^{i+m-1} \mathsf{C}^b( \ . \ )'_{j^b} + \mathsf{B}( \ . \ )'_{i+m} \Big], \tag{3.1}$$

where

$$\begin{gathered} m = \frac{(\ell_f)_i}{\Delta x} \geq 2, \quad \mathsf{A} = \frac{\Gamma(2-\alpha)}{2\Gamma(2)\Gamma(3-\alpha)}, \quad \mathsf{B} = (m-1)^{2-\alpha} - (m+\alpha-2)m^{1-\alpha}, \\ \mathsf{C}^a = (i-j^a+1)^{2-\alpha} - 2(i-j^a)^{2-\alpha} + (i-j^a-1)^{2-\alpha}, \\ \mathsf{C}^b = (j^b-i+1)^{2-\alpha} - 2(j^b-i)^{2-\alpha} + (j^b-i-1)^{2-\alpha}. \end{gathered} \tag{3.2}$$

Thus, Eq. (3.2) represents the fractional derivative by the weighted sum of the first-order derivatives at the points $(i-m) \div (i+m)$ with appropriate weight coefficients marked as $\mathsf{B}$, $\mathsf{C}^a$ and $\mathsf{C}^b$. The first-order derivative is then approximated by the finite difference method. Scilab and Julia programming languages were used in the implementation.

The numerical models corresponding to the governing equations are presented in detail in Section 3 of the **Publication A.1÷Publication A.5**.

## 3.2 Parametric study

Firstly, it should be pointed out that fractional structural models are described by two additional parameters ($\alpha$ and $\ell_f$) compared to their classical counterparts, thus fulfilling the stated **Requirement R.1**. Secondly, as mentioned using $\alpha = 1.0$, one always obtains governing equations identical to the classical formulations. Finally, this subsection aims to examine how changes in new parameters affect the behavior of fractional structural models (deflections, eigenfrequencies, modes, and plastic hinges formation). Only selected representative results are presented below, as the overall insights and conclusions are the same for all fractional models contained in the dissertation.

Accordingly, Fig. 3.1 shows deflections of a fractional structural element. In this example, these are the deflections of the s-FKLP model for square micro-plate with dimensions $L_{x_1} = L_{x_2} = L = 10\ \mu m$ and thickness $t = 0.25\ \mu m$ and a uniformly distributed load $p_3 = -0.01\ \frac{\mu N}{\mu m^2}$. Next, Fig. 3.2 shows dimensionless frequency $\bar{f} = \frac{\omega}{2\pi}\frac{L^2}{\pi^2}\sqrt{\frac{\rho A}{EI}}$ and shape of the first mode for the s-FTB model for the fixed beam with length to height ratio $L/b = 2$ and Poisson's ratio $\nu = 0.2$, for $\alpha \in \{0.9, 0.7\}$ and $\ell_f^{max} \in \{0.001L, 0.1L, 0.2L\}$ compared to the results of classical Timoshenko beam (CTB) model (s-FTB model with $\alpha = 1.0$) and the results of s-FEBB model with $\alpha = 0.7$. Next, Table 3.1 contains the maximum value of the external mid-point load $F_{el}$ to be carried by the fixed beam in elastic state and the load value $F_{pl}$ at a total strain of 3%, according to the s-FEBB/s-FTB model and the corresponding plastic zone.

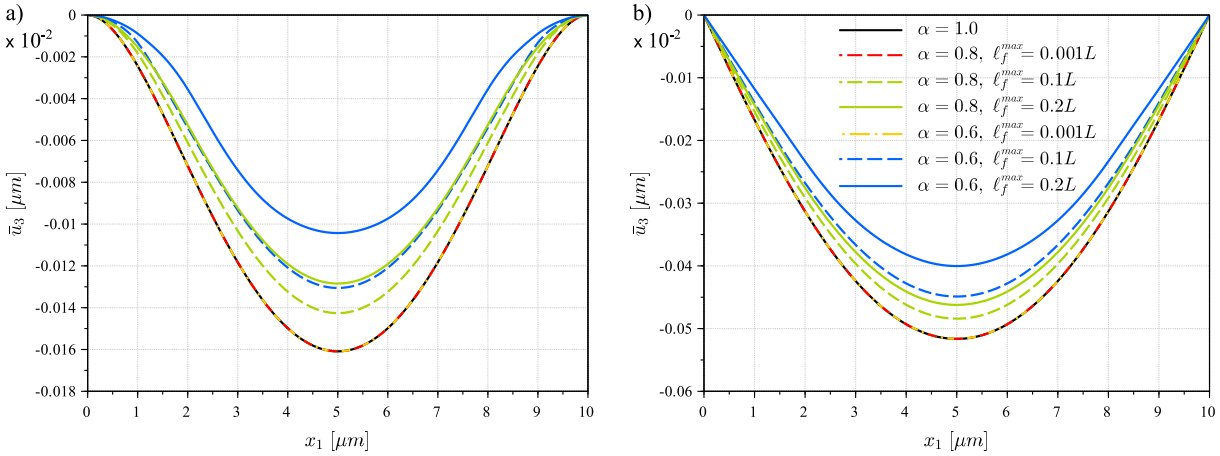


**Figure 3.1:** Deflection of plate predicted by s-FKLP model with uniformly distributed load, for $\alpha \in \{0.8, 0.6\}$, $\ell_f^{max} \in \{0.001L, 0.10L, 0.20L\}$ vs. deflection of CKLP model (i.e. $\alpha = 1.0$); for the following boundary conditions a) CCCC, b) SSSS. Reprinted from **Publication A.5** [34].

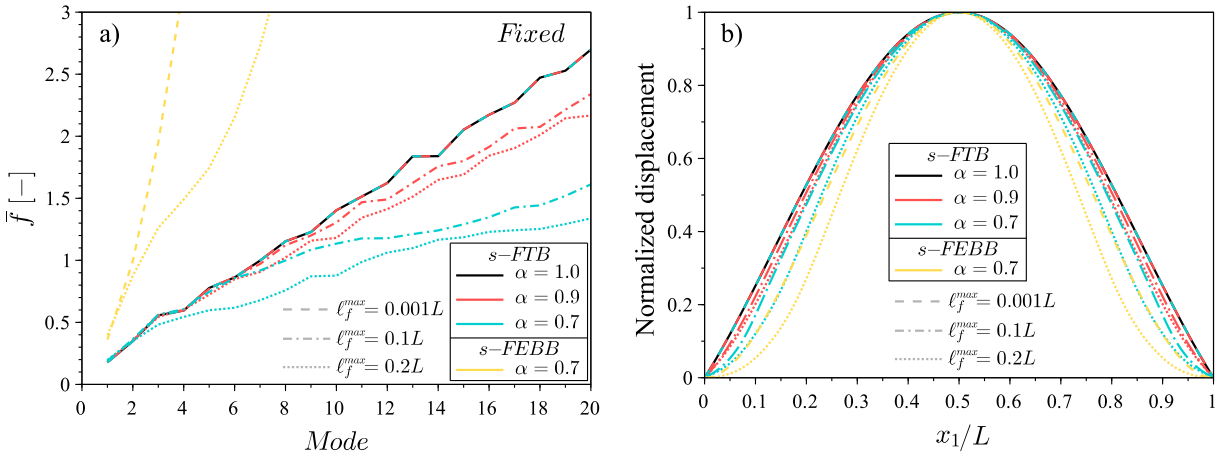


**Figure 3.2:** a) Dimensionless frequency $\bar{f}$ and b) shape of first mode; for the s-FTB model for the fixed beam with length to height ratio $L/b = 2$ and Poisson's ratio $\nu = 0.2$, for $\alpha \in \{0.9, 0.7\}$ and $\ell_f^{max} \in \{0.001L, 0.1L, 0.2L\}$ compared to the results of CTB model (s-FTB model with $\alpha = 1.0$) and the results of s-FEBB model with $\alpha = 0.7$. Reprinted from **Publication A.3** [31].

For more examples, the reader is referred to the **Publication A.1** (s-FEBB model), **Publication A.2** (s-FTB model) and **Publication A.5** (s-FKLP model) - for results of static elastic bending; to the **Publication A.4** (s-FEBB and s-FTB models) - for results of static elastic-plastic bending; to the **Publication A.3** (s-FEBB and s-FTB models) - for results of free vibrations.

**Summarily, the following findings are drawn from the parametric study:**

- parameters $\alpha$ and $\ell_f$ influence the deflections, frequency values, and shape of modes of the fractional models of a structural element;
- the non-locality effect disappears if the dimensions of the structural elements are much larger than the length scale ($\ell_f^{max} = 0.001L$), regardless of $\alpha$ and type of analysis (statics/dynamics). The results are then highly similar to the classical formulation ($\alpha = 1.0$), which fulfills **Requirement R.2**. Therefore, for a body with a very fine microstructure (relative to the body dimensions), it is applicable to use the classical models of structural elements as a special case of the non-local formulation;
- if the dimensions of the structural element and the length scale are of similar size order (in the examples presented, it is $\ell_f^{max} = \{0.1L;\ 0.2L\}$), ignoring the discontinuous (granular) microstructure is incorrect, as the scale effect is significant. The lower the value of $\alpha$ or the larger $\ell_f$, the stronger the scale effect is observed;

**Table 3.1:** The maximum value of the external mid-point load $F_{el}$ to be carried by the fixed beam in elastic state and the load value $F_{pl}$ at a total strain of 3%, according to the s-FEBB/s-FTB model and the corresponding plastic zone. Reprinted from **Publication A.4** [32].

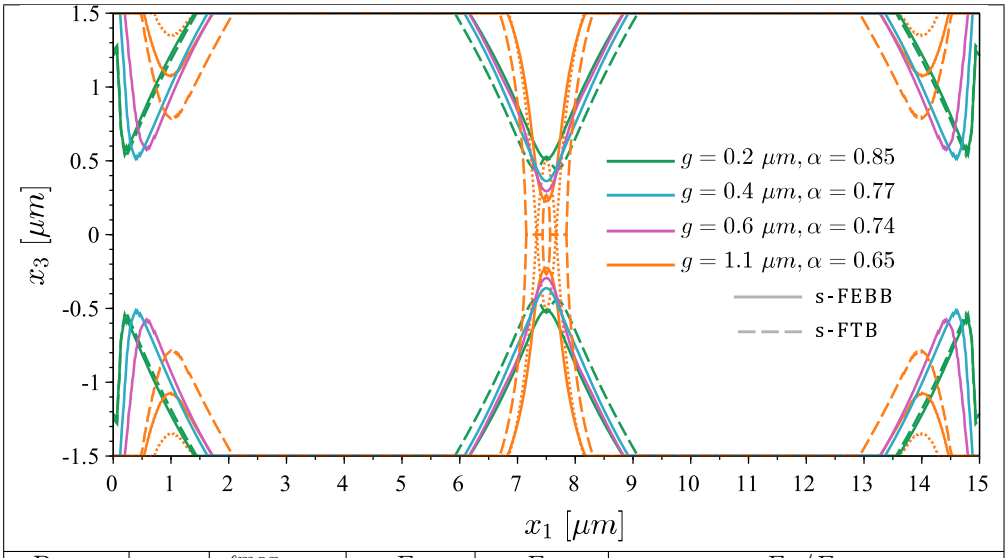


| Beam model | $\alpha$ [−] | $\ell_f^{max} = g$ $[\mu m]$ | $F_{el}$ $[\mu N]$ | $F_{pl}$ $[\mu N]$ | $F_{pl}/F_{el}$ [−] |
|---|---|---|---|---|---|
| s-FEBB | 0.85 | 0.2 | 9768.84 | 14988.40 | 1.534 |
| s-FTB | | | 9703.24 | 14474.83 | 1.492 |
| s-FEBB | 0.77 | 0.4 | 6810.48 | 11376.22 | 1.670 |
| s-FEBB | 0.74 | 0.6 | 5433.44 | 9372.87 | 1.725 |
| s-FEBB | 0.65 | 1.1 | 3429.56 | 6395.64 | 1.865 |
| s-FTB | | | 3410.06 | 5422.06*<br>6418.63 | 1.590<br>1.882 |
| *1st plastic hinge at total strain 1.42% (dotted line) | | | | | |

- the distribution of the plastic zone depends not only on the boundary conditions and load conditions but also on the microstructure (characterized by $\alpha$ and $\ell_f$);
- the ratio of the load in the plastic state ($F_{pl}$) to the one in the elastic state ($F_{el}$)is higher for microstructures of larger grains, but simultaneously the plastification of the first fibers (yield stress according to the Hall-Petch relationship) occurs at a lower load value. Hence, the load-carrying ability of beams with a coarse-grained microstructure is lower than that of a fine-grained one. The non-locality is also revealed by changing the distribution of plastic zones.

Since the s-FTB model is more general than the s-FEBB one, in **Publication A.2**, **Publication A.3** and **Publication A.4**, the differences in results are indicated as well as when the simpler s-FEBB model can be reasonably used. Fig. 3.3a shows a comparison of the maximum deflections for these models, while Fig. 3.3b compares the frequencies - depending on the beam length to height $L/b$ ratio. In **Publication A.5**, a similar comparison is made between a two-dimensional element (plate) and a one-dimensional element (beam). Fig. 3.4 shows a comparison of the maximum deflections for these models - depending on the ratio of its length to width $\frac{L_{x_1}}{L_{x_2}}$.

**Summarily, the following findings are drawn from the aforementioned comparisons of space-fractional models:**

- There is a need to consider the shear effect (and the rotational inertia) when the beam is thick in relation to its length.
- For beams with a high ratio of beam length to cross-section height $L/b$, the s-FTB model can be reduced to the s-FEBB model without losing the correctness of the results - which is analogical to

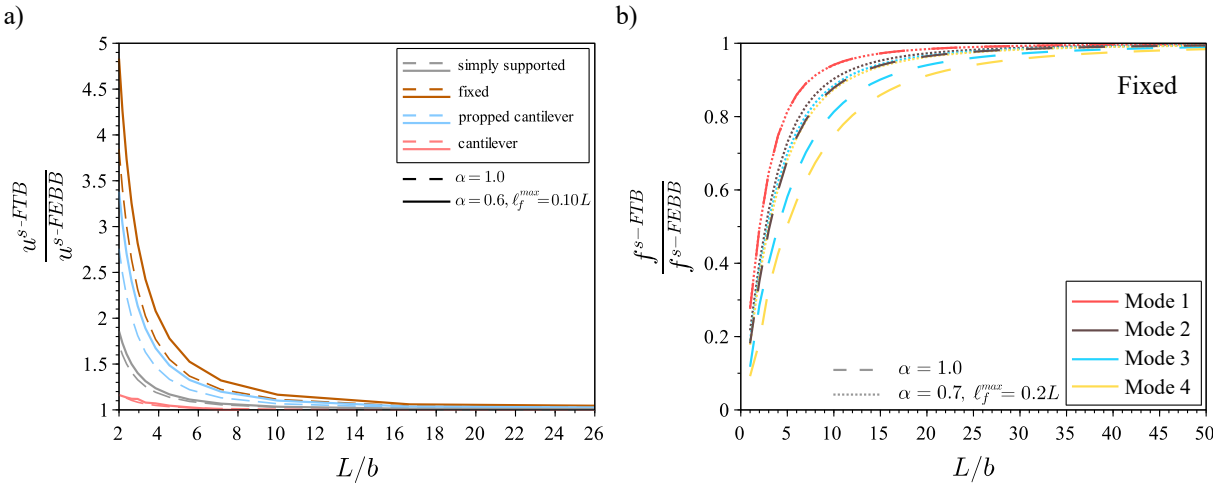


**Figure 3.3:** Comparison of s-FTB and s-FEBB models in the case of a) maximum deflection for the simply supported scheme, the fixed scheme, and the propped cantilever scheme with mid-span point load and the cantilever scheme with end-point load, for $\alpha = 0.6$, $\ell_f^{max} = 0.10L$. Reprinted from **Publication A.2** [30]; b) the frequency value of first four modes for the fixed scheme and $\alpha = 0.7$, $\ell_f^{max} = 0.2L$. Reprinted from **Publication A.3** [31].

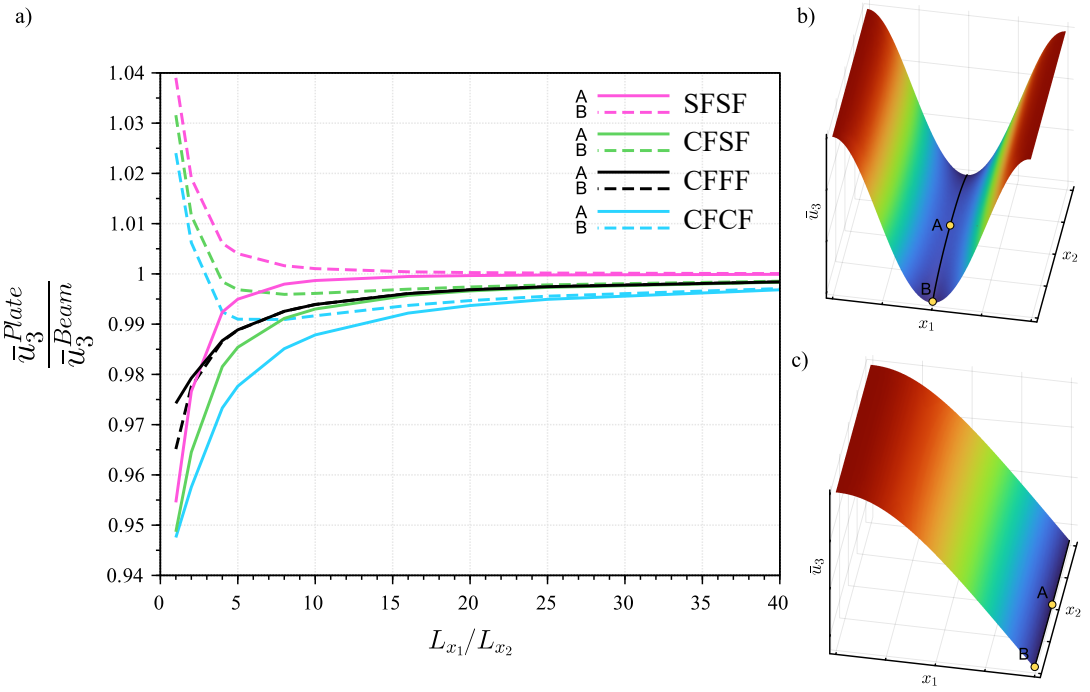


**Figure 3.4:** (a) Comparison of deflections by s-FKLP and s-FEBB models, loaded with uniformly distributed load, CFCF, SFSF, CFSF, CFFF; (b) location of points A and B for schemes SFSF, CFSF, CFCF, and (c) CFFF. Reprinted from **Publication A.5** [34].

local Timoshenko and Euler-Bernoulli beams.

- The shear effect for small-scale thick beams should be considered for a higher ratio $L/b$ than in local theory (the inclusion of the non-locality makes the shear effect more significant than in the classic approach) in the case of static bending (see Fig. 3.3a).
- However, in the case of free vibrations, the shear effect for small-scale thick beams can be considered for a lower ratio $L/b$ than in local theory (the inclusion of the non-locality makes the shear effect less significant than in the classic approach) (see Fig. 3.3b).
- For higher frequencies, the s-FEBB can be used reasonably and without loss of correctness only for significantly slender beams in comparison to statics.
- Shear strains have a negligible influence on the formation of the plastic zone in the case of the

simply supported beam. However, for a fixed beam - regardless of the load conditions - in the case of the Timoshenko beam, for the same level of deformation as in the case of the Euler-Bernoulli beam, a larger part of the beam becomes plasticized. The load capacity ($F_{el}$, $F_{pl}$, $p_{el}$, $p_{pl}$) of s-FTB is smaller than that of s-FEBB, and the inclusion of shear deformation leads to the formation of a full plastic hinge at a lower load level.

- The beam model has a limitation related to boundary conditions, which can be applied only to opposite ends of the structure described by this model. In contrast, the plate model allows for more combinations of boundary conditions, including those not possible in one-dimensional beam models, such as the supporting of all edges. This advantage of plate models over beam models makes the s-FKLP formulation a more versatile approach to modeling structures.

## 3.3 Validation

At the outset, it is sought to emphasize that the non-local parameters of the model ($\alpha$ and $\ell_f$) are considered in each case as material parameters, and more specifically as related to the microstructure of the specific material. In **Publication A.4**, it is identified that one of the parameters (length scale) is equal to the grain size of the microstructure $g$, which fulfills **Requirement R.3**. Fig. 3.5 presents the comparison of experimental measurements (stress–strain relation) from compression test of WC-Co micropillars [36] with different grain sizes and results of the space-Fractional 1D (truss) model. Fig. 3.6 shows tested micropillars with different grain sizes [36].

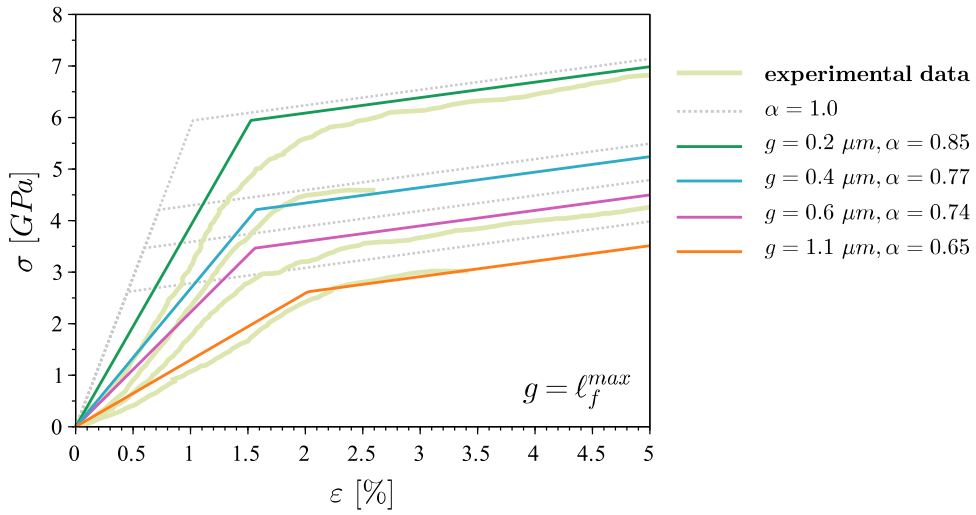


**Figure 3.5:** The comparison of experimental measurements (stress–strain relation) from compression test of WC-Co tapered micropillars [36] vs. classical model ($\alpha = 1.0$), vs. space-Fractional 1D model. Reprinted from **Publication A.4** [32].

The main goal of the doctoral dissertation was to create models that represent real nano/micro-sized structural elements, and in this regard, the results of the validations of the s-FEBB, s-FTB, and s-FKLP models are presented below to ensure that fractional models meet the stated aim of providing results consistent with real objects. Only selected validation results are presented below in the graphical form, while details of the validations are provided in **Publications A.1÷A.5**, and the reader is referred to there. In each case, the results obtained according to the space-fractional model and the classical model are shown. The validation involved:

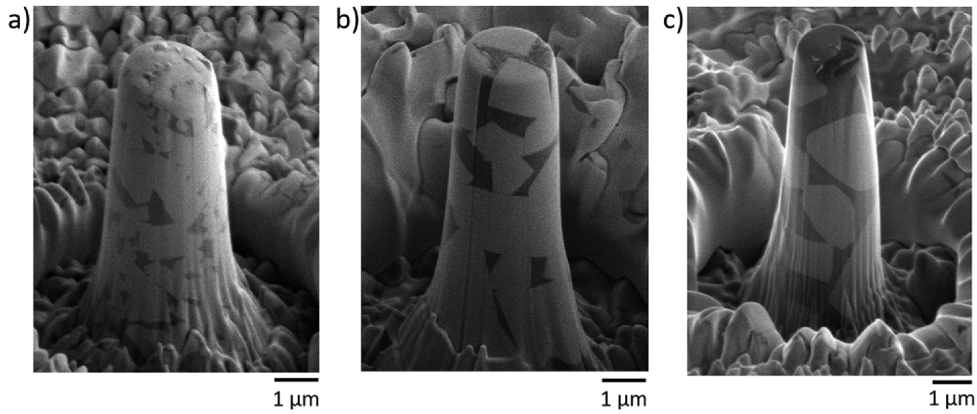


**Figure 3.6:** Images of micropillars with different grain sizes [36]. Reprinted from *Sandoval et al. Influence of specimen size and microstructure on uniaxial compression of WC-Co micropillars. Ceramics International, 2019, 45, 15934-15941*, Copyright (2019), with permission from Elsevier.

- **Publication A.1** - s-FEBB model based on the bending test of silver nano-beams (experimental data from [3]).

  Fig. 3.7 presents the comparison of deflection for the s-FEBB model, the classical model (CEBB), and experimental measurement. The static scheme is the fixed beam (Fig. 3.7a) and the simply supported beam (Fig. 3.7b). During the validation, 4 different bending tests from the experiment were reproduced numerically.

  Although the nano-beams have different geometrical dimensions (length $L$ and diameter $d$ of circular cross-section) and different support schemes, it was possible to establish a single set of parameters ($\alpha = 0.8$ and $\ell_f = 160\ nm$).

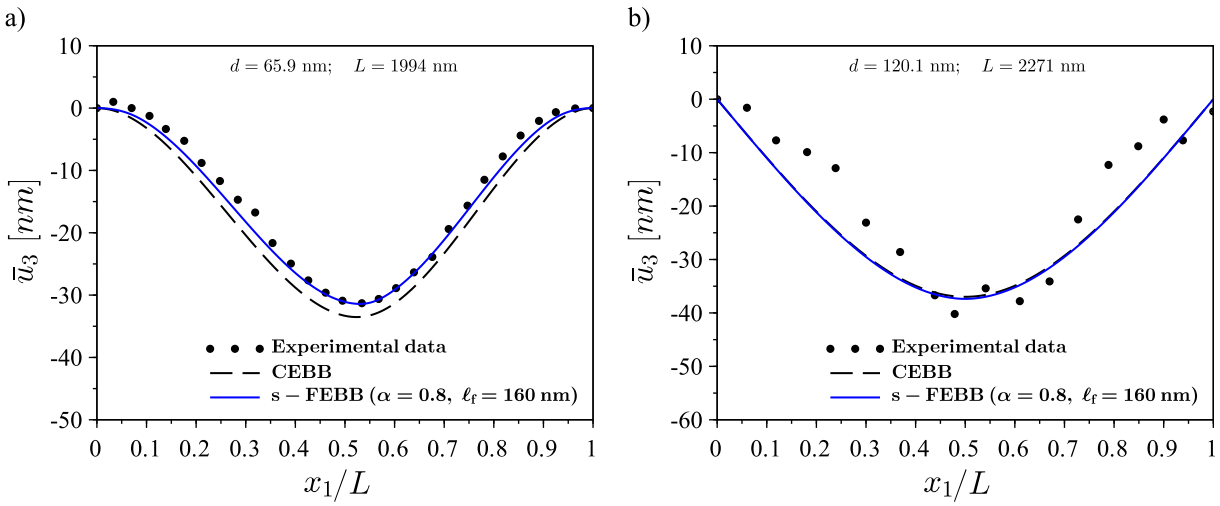


**Figure 3.7:** The comparison of experimental measurements [3] (deflections) of silver nano-beams vs. classical model (CEBB) and s-FEBB model for the a) fixed beam; b) simply supported beam, loaded by a point load. Reprinted from **Publication A.1** [29].

- **Publication A.2** - s-FTB model based on the bending test of SU-8 polymer micro-cantilevers (experimental data from [37]).

  Fig. 3.8 presents the bending results of the micro-cantilevers in the form of an elastic modulus calculated from the deflections as for the local Timoshenko beam theory for a cantilever with a point load $F$ at the free end,

$$E = \left(\frac{FL^3}{3I} + \frac{2(1+\nu)FL}{kA}\right)\bar{u}_3. \tag{3.3}$$

During the validation, 27 different bending tests from the experiment were reproduced numerically. Although the micro-cantilevers have different geometrical dimensions (length and size of rectangular cross-section), it was possible to establish a single set of parameters ($\alpha = 0.75$ and $\ell_f = 5\ \mu m$).

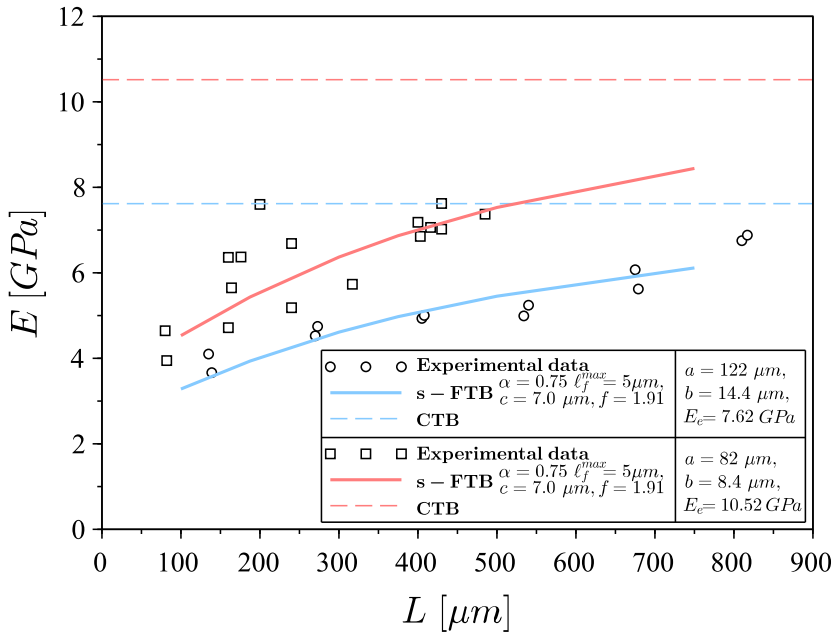


**Figure 3.8:** The comparison of experimental measurements [37] (elastic modulus) of SU-8 polymer micro-cantilevers loaded at the free end, vs. the results of the s-FTB model and CTB model. Reprinted from **Publication A.2** [30].

- **Publication A.3** - s-FEBB model based on the bending test and resonance of GaN nano-beams (experimental data from [38] and [39], respectively);

  Fig. 3.9a presents the results of beam bending (predicted deflections), while Fig. 3.9b presents the results of resonance analysis (predicted resonance frequencies to experimental measurements ratio $\frac{f^{s-FEBB}}{f^{EXP}}$). During the validation, 12 different tests (4 for static bending and 8 for resonance) from the experiment were reproduced numerically.

  Although the nano-beams have different cross-sectional shapes and sizes, and different lengths, as well as involving different tests - bending (statics) and resonant oscillations (dynamics), it was possible to establish a single set of parameters ($\alpha = 0.66$ and $\ell_f = 160\ nm$).

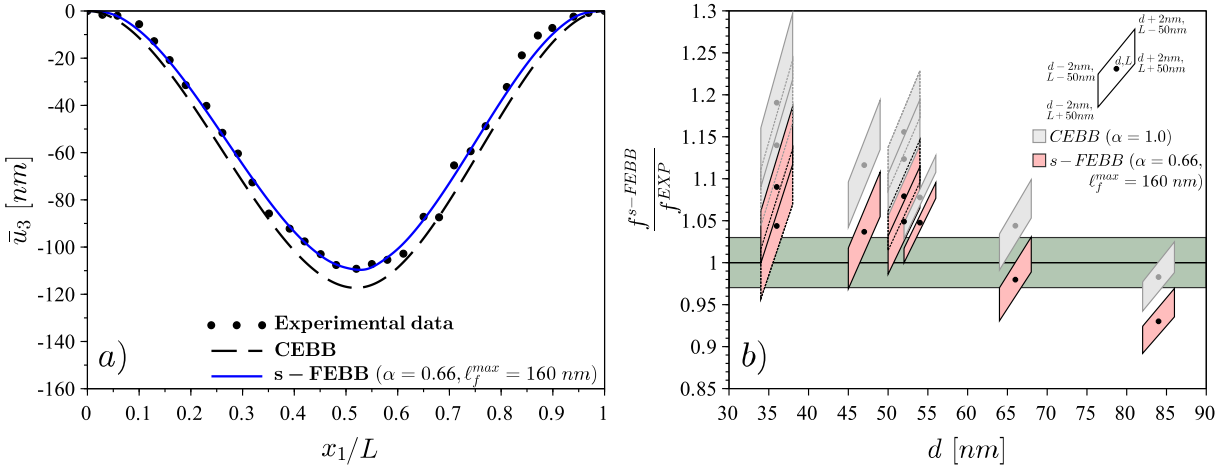


**Figure 3.9:** The comparison of experimental measurements a) deflections $\bar{u}_3$ [38] and b) resonance frequencies $f^{EXP}$ [39] of GaN nanobeams vs. classical model (CEBB) and s-FEBB model. Reprinted from **Publication A.3** [31].

- **Publication A.5** - s-FKLP model based on the bending test of composite micro-plates (experimental data from [40]).

  Fig. 3.9 presents the results of the micro-plate bending test in the form of stiffness

$$S_b = \frac{F}{\bar{u}_F}, \tag{3.4}$$

  where $\bar{u}_F$ is a displacement under the point load $F$. The static scheme is the cantilever plate. During the validation, 11 different bending tests from the experiment were reproduced numerically. Although the micro-plates have different geometrical dimensions (length $L$), it was possible to establish a single set of parameters ($\alpha = 0.5$ and $\ell_f = 0.48\ \mu m$).

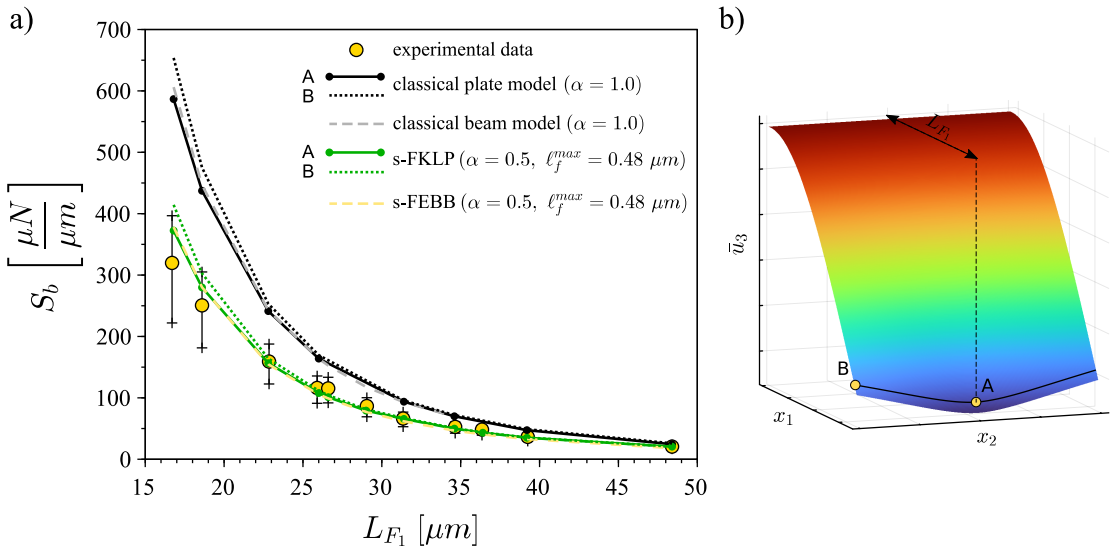


**Figure 3.10:** The comparison of experimental results (stiffness $S_b$) from bending test of sandwich micro-plates [40] vs. results of the classical plate and beam models ($\alpha = 1.0$) vs. results of s-FKLP and s-FEBB models (; $L_{F_1}$ is the load position and the plate length is $L_{x_1} = L_{F_1} + 0.4\ \mu m$); b) location of points A and B. Reprinted from **Publication A.5** [34].

**Summarily, the following findings are drawn from the aforementioned validations of space-fractional models:**

- Classical (local) structural models are unable to cover experimental data from tests of nano/micro-size elements.
- The results of the space-fractional models are closer to the experimental data than the classical (local) CM ones which fulfills stated **Requirement R.4**.
- Space-Fractional structural models allow input of the same non-local parameters regardless of whether static or dynamic equilibrium is considered.
- The non-local parameters do not depend on the geometry of the structural element or the support conditions, but only on the material it is made of (specifically, the length scale $\ell_f$ depends on the characteristic dimension of the microstructure - the grain size).

# 4

# Conclusions

## 4.1 Final remarks

The aim of this dissertation was to develop structural models that take into account scale effects to predict the mechanical response of structural elements over scales to a given external load. To achieve the stated aim, it was posed that the use of the fractional derivative will allow the introduction of non-locality. The following procedure was undertaken:

- The non-local fractional structural elements were formulated as a generalization of classical structural elements, utilizing fractional calculus. The subjects of the research were basic structural elements such as beams and plates with scale effects. A total of eight structural models were eventually developed in the framework of space-Fractional Continuum Mechanics:
  - space-Fractional Euler-Bernoulli Beam (s-FEBB) - for static elastic bending; static elastic-plastic bending; free vibrations.
  - space-Fractional Timoshenko Beam (s-FTB) - for static elastic bending; static elastic-plastic bending; free vibrations.
  - space-Fractional Kirchhoff-Love Plate (s-FKLP) - for static elastic bending.
  - space-Fractional Mindlin-Reissner Plate (s-FMRP) - for static elastic bending.

  In Section 2, the governing equations for these models are presented.
- The models were implemented using numerical methods (Section 3.1) to make finding a solution computationally efficient and convenient for applications in engineering computing.
- A parametric study was conducted to show how changes in new parameters affect the behavior of fractional structural models (deflections, eigenfrequencies, modes, and plastic hinges formation). Specific findings drawn from the parametric study are provided in Section 3.2.
- Validations were conducted to prove that space-fractional models provide results consistent with real objects (Section 3.3).

The most important features of the developed fractional models are the following:

- There are only two additional parameters ($\alpha$ and $\ell_f$) compared to their classical counterparts. These parameters control the scale effect in models.
- If the external characteristic length (structural element size) is much larger than the internal one (e.g. grain size), then the results of non-local continuum models align with the results of classical continuum models. On the other hand, if $\alpha = 1.0$ is given, space-fractional models revert directly to their classical (local) form.
- New model parameters are associated with the microstructure of the material (especially length scale $\ell_f$ was established as equal to grain size). Consequently, a single set of parameters in statics and dynamics is obtained, which was unreachable in competitive non-local models.

- Most importantly, models have the ability to provide a good approximation of experimental results for nano/micro-beams and nano/micro-plates.

**Based on the above, one can state that the aim of the dissertation, which was *to develop structural models that take into account scale effects to predict the mechanical response of structural elements to a given external load*, has been achieved, and the thesis stated that *the use of the fractional derivative introduces the non-locality into structural mechanical models, allowing to capture scale effect* was correct.**

## 4.2 Future tasks

The research contained in the dissertation continues under Grant No. 2022/45/N/ST8/02421 entitled *Mechanics of bar-and-plate structures with strong scale effects - mathematical modelling and experimental analysis* funded in the period 04.2023-03.2026 by the National Science Centre, Poland. The research will be concerned with investigating and describing the mechanical behavior of complex small-scale structures such as nano/micro-trusses, nano/micro-frames, and nano/micro-sized beam-plate systems. Achievements from the dissertation will be used, as the complex structure will be treated as a system of base elements (space-fractional beams, space-fractional plates) connected together. Therefore, in the future, the results obtained may constitute the base for the development of appropriate tools for the optimal design of structures in which scale effects occur (e.g., components in nano- and micro-devices).

In addition, the availability of different types of fractional derivatives leads to the questions: How would using a different type of derivative (than the Riesz-Caputo derivative used in the dissertation) affect the results, and should the type of derivative be selected depending on the class of materials?

Further future tasks may also involve expanding the models to include aspects that were left out of the dissertation:

- consideration of axial forces;
- consideration of damping effects in dynamics;
- use of other numerical methods, such as the finite element method.

# Bibliography


[1] S. Timoshenko and J. Goodier, *Theory of Elasticity*. Engineering societies monographs, McGraw-Hill, 1951. [cited at p. 1]

[2] M. N. Esfahani and B. E. Alaca, "A review on size-dependent mechanical properties of nanowires," *Advanced Engineering Materials*, vol. 21, no. 8, p. 1900192, 2019. [cited at p. 1]

[3] Y. Chen, B. L. Dorgan, D. N. McIlroy, and D. E. Aston, "On the importance of boundary conditions on nanomechanical bending behavior and elastic modulus determination of silver nanowires," *Journal of Applied Physics*, vol. 100, no. 10, p. 104301, 2006. [cited at p. 1, 18]

[4] J. Hu, X. W. Liu, and B. C. Pan, "A study of the size-dependent elastic properties of ZnO nanowires and nanotubes," *Nanotechnology*, vol. 19, no. 28, p. 285710, 2008. [cited at p. 1]

[5] V. Gryaznov and L. Trusov, "Size effects in micromechanics of nanocrystals," *Progress in Materials Science*, vol. 37, no. 4, pp. 289–401, 1993. [cited at p. 1]

[6] D. J. Young, C. A. Zorman, and M. Mehregany, "MEMS/NEMS devices and applications," in *Springer Handbook of Nanotechnology*, pp. 359–387, Springer Berlin Heidelberg, 2010. [cited at p. 1]

[7] T. Burczyński, M. Pietrzyk, W. Kuś, L. Madej, A. Mrozek, and L. Rauch, *Multiscale modelling and optimization of materials and structures*. Hoboken, NJ: Wiley, 2022. [cited at p. 1]

[8] M. Shaat, E. Ghavanloo, and S. A. Fazelzadeh, "Review on nonlocal continuum mechanics: Physics, material applicability, and mathematics," *Mechanics of Materials*, vol. 150, p. 103587, 2020. [cited at p. 1, 2]

[9] A. C. Eringen, "On differential equations of nonlocal elasticity and solutions of screw dislocation and surface waves," *Journal of Applied Physics*, vol. 54, no. 9, pp. 4703–4710, 1983. [cited at p. 2]

[10] R. Mindlin and N. Eshel, "On first strain-gradient theories in linear elasticity," *International Journal of Solids and Structures*, vol. 4, no. 1, pp. 109–124, 1968. [cited at p. 2]

[11] G. Romano and R. Barretta, "Stress-driven versus strain-driven nonlocal integral model for elastic nano-beams," *Composites Part B: Engineering*, vol. 114, pp. 184–188, 2017. [cited at p. 2]

[12] A. K. Lazopoulos, "On fractional peridynamic deformations," *Archive of Applied Mechanics*, vol. 86, no. 12, pp. 1987–1994, 2016. [cited at p. 2]

[13] A. C. Eringen, "Linear theory of micropolar elasticity," tech. rep., 1965. [cited at p. 2]

[14] A. Farajpour, M. H. Ghayesh, and H. Farokhi, "A review on the mechanics of nanostructures," *International Journal of Engineering Science*, vol. 133, pp. 231–263, 2018. [cited at p. 2]

[15] A. A. Nuhu and B. Safaei, "State-of-the-art of vibration analysis of small-sized structures by using nonclassical continuum theories of elasticity," *Archives of Computational Methods in Engineering*, 2022. [cited at p. 2]

[16] M. A. Khorshidi, "The material length scale parameter used in couple stress theories is not a material constant," *International Journal of Engineering Science*, vol. 133, pp. 15–25, 2018. [cited at p. 2]

[17] M. Shariati, B. Azizi, M. Hosseini, and M. Shishesaz, "On the calibration of size parameters related to non-classical continuum theories using molecular dynamics simulations," *International Journal of Engineering Science*, vol. 168, p. 103544, 2021. [cited at p. 2]

[18] W. Chan and H. Chen, "Modeling material length-scale effect using the second-order peridynamic material correspondence model," *International Journal of Engineering Science*, vol. 189, p. 103877, 2023. [cited at p. 2]

[19] H. T. Davis, "The application of fractional operators to functional equations," *American Journal of Mathematics*, vol. 49, no. 1, p. 123, 1927. [cited at p. 3]

[20] I. Podlubny, *Fractional differential equations : an introduction to fractional derivatives, fractional differential equations, to methods of their solution and some of their applications*. San Diego: Academic Press, 1999. [cited at p. 7]

[21] J. Leszczyński, *An introduction to fractional mechanics*. Monographs No 198, The Publishing Office of Czestochowa University of Technology, 2011. [cited at p. 7, 13]

[22] G. S. Teodoro, J. T. Machado, and E. C. de Oliveira, "A review of definitions of fractional derivatives and other operators," *Journal of Computational Physics*, vol. 388, pp. 195–208, 2019. [cited at p. 7]

[23] W. Sumelka, "Thermoelasticity in the framework of the fractional continuum mechanics," *Journal of Thermal Stresses*, vol. 37, no. 6, pp. 678–706, 2014. [cited at p. 7]

[24] W. Sumelka and T. Blaszczyk, "Fractional continua for linear elasticity," *Archives of Mechanics*, vol. 66, no. 3, pp. 147–172, 2014. [cited at p. 7]

[25] W. Sumelka, "On geometrical interpretation of the fractional strain concept," *Journal of Theoretical and Applied Mechanics*, apr 2016. [cited at p. 8]

[26] K. Szajek and W. Sumelka, "Discrete mass-spring structure identification in nonlocal continuum space-fractional model," *The European Physical Journal Plus*, vol. 134, no. 9, 2019. [cited at p. 8]

[27] W. Sumelka, "On fractional non-local bodies with variable length scale," *Mechanics Research Communications*, vol. 86, pp. 5–10, 2017. [cited at p. 8]

[28] O. A. Bauchau and J. I. Craig, eds., *Structural Analysis*. Springer Netherlands, 2009. [cited at p. 8, 10]

[29] P. Stempin and W. Sumelka, "Space-fractional Euler-Bernoulli beam model - theory and identification for silver nanobeam bending," *International Journal of Mechanical Sciences*, vol. 186, p. 105902, 2020. [cited at p. 9, 18]

[30] P. Stempin and W. Sumelka, "Formulation and experimental validation of space-fractional timoshenko beam model with functionally graded materials effects," *Computational Mechanics*, vol. 68, no. 3, pp. 697–708, 2021. [cited at p. 9, 16, 19]

[31] P. Stempin and W. Sumelka, "Dynamics of space-fractional euler–bernoulli and timoshenko beams," *Materials*, vol. 14, no. 8, p. 1817, 2021. [cited at p. 9, 14, 16, 19]

[32] P. Stempin and W. Sumelka, "Space-fractional small-strain plasticity model for microbeams including grain size effect," *International Journal of Engineering Science*, vol. 175, p. 103672, 2022. [cited at p. 10, 15, 17]

[33] S. Aydinlik, A. Kiris, and W. Sumelka, "Three-dimensional analysis of nonlocal plate vibration in the framework of space-fractional mechanics — theory and validation," *Thin-Walled Structures*, vol. 163, p. 107645, 2021. [cited at p. 10, 12]

[34] P. Stempin, T. P. Pawlak, and W. Sumelka, "Formulation of non-local space-fractional plate model and validation for composite micro-plates," *International Journal of Engineering Science*, vol. 192, p. 103932, 2023. [cited at p. 11, 14, 16, 20]

[35] Z. Odibat, "Approximations of fractional integrals and caputo fractional derivatives," *Applied Mathematics and Computation*, vol. 178, no. 2, pp. 527–533, 2006. [cited at p. 13]

[36] D. Sandoval, A. Rinaldi, A. Notargiacomo, O. Ther, E. Tarrés, J. Roa, and L. Llanes, "Influence of specimen size and microstructure on uniaxial compression of WC-co micropillars," *Ceramics International*, vol. 45, no. 13, pp. 15934–15941, 2019. [cited at p. 17, 18]

[37] C. Liebold, "Größeneffekt in der elastizität," 2015. [cited at p. 18, 19]

[38] Y. Chen, I. Stevenson, R. Pouy, L. Wang, D. N. McIlroy, T. Pounds, M. G. Norton, and D. E. Aston, "Mechanical elasticity of vapour–liquid–solid grown GaN nanowires," *Nanotechnology*, vol. 18, no. 13, p. 135708, 2007. [cited at p. 19]

[39] C.-Y. Nam, P. Jaroenapibal, D. Tham, D. E. Luzzi, S. Evoy, and J. E. Fischer, "Diameter-dependent electromechanical properties of GaN nanowires," *Nano Letters*, vol. 6, no. 2, pp. 153–158, 2006. [cited at p. 19]

[40] S. P. Baker and W. D. Nix, "Mechanical properties of compositionally modulated au-ni thin films: Nanoindentation and microcantilever deflection experiments," *Journal of Materials Research*, vol. 9, no. 12, pp. 3131–3144, 1994. [cited at p. 20]

# Appendices

# A

# Publications

## A.1 Publication 1

**P. Stempin** and W. Sumelka. *Space-fractional Euler-Bernoulli beam model - Theory and identification for silver nanobeam bending.* International Journal of Mechanical Sciences, 2020, 186, 105902.
($IF_{2020} = 5.329$)
DOI: 10.1016/j.ijmecsci.2020.105902

**Abstract**

This paper is concentrated on the non-local bending analysis of nanobeams and the improvement of the space-Fractional Euler-Bernoulli beam (s-FEBB) theory. A new kinematics is proposed for s-FEBB and a numerical algorithm is developed to enable the introduction of a variable length scale, arbitrary boundary conditions, and arbitrary transverse load conditions. The obtained results indicate that the scale effect depends on boundary conditions and the distribution of the length scale as well as the order of fractional continua. Moreover, the identification and validation based on silver nanobeam bending experimental tests confirmed the capability of the proposed fractional model to capture the measurements.

## A.2 Publication 2

**P. Stempin** and W. Sumelka. *Formulation and experimental validation of space-fractional Timoshenko beam model with functionally graded materials effects.* Computational Mechanics, 2021, 68, 697-708.
($IF_{2021} = 4.391$)
DOI: 10.1007/s00466-021-01987-6

**Abstract**

In this study, the static bending behaviour of a size-dependent thick beam is considered including FGM (Functionally Graded Materials) effects. The presented theory is a further development and extension of the space-fractional (non-local) Euler–Bernoulli beam model (s-FEBB) to space-fractional Timoshenko beam (s-FTB) one by proper taking into account shear deformation. Furthermore, a detailed parametric study on the influence of length scale and order of fractional continua for different boundary conditions demonstrates, how the non-locality affects the static bending response of the s-FTB model. The differences in results between s-FTB and s-FEBB models are shown as well to indicate when shear deformations need to be considered. Finally, material parameter identification and validation based on the bending of SU-8 polymer microbeams confirm the effectiveness of the presented model.

## A.3 Publication 3

**P. Stempin** and W. Sumelka. *Dynamics of Space-Fractional Euler–Bernoulli and Timoshenko Beams.* Materials, 2021, 14, 1817. ($IF_{2021} = 3.748$)
DOI: 10.3390/ma14081817

**Abstract**

This paper investigates the dynamics of the beam-like structures whose response manifests a strong scale effect. The space-Fractional Euler–Bernoulli beam (s-FEBB) and space-Fractional Timoshenko beam (s-FTB) models, which are suitable for small-scale slender beams and small-scale thick beams, respectively, have been extended to a dynamic case. The study provides appropriate governing equations, numerical approximation, detailed analysis of free vibration, and experimental validation. The parametric study presents the influence of non-locality parameters on the frequencies and shape of modes delivering a depth insight into a dynamic response of small scale beams. The comparison of the s-FEBB and s-FTB models determines the applicability limit of s-FEBB and indicates that the model (also the classical one) without shear effect and rotational inertia can only be applied to beams significantly slender than in a static case. Furthermore, the validation has confirmed that the fractional beam model exhibits very good agreement with the experimental results existing in the literature—for both the static and the dynamic cases. Moreover, it has been proven that for fractional beams it is possible to establish constant parameters of non-locality related to the material and its microstructure, independent of beam geometry, the boundary conditions, and the type of analysis (with or without inertial forces).

## A.4 Publication 4

**P. Stempin** and W. Sumelka. *Space-fractional small-strain plasticity model for microbeams including grain size effect*. International Journal of Engineering Science, 2022, 175, 103672. ($IF_{2022} = 6.600$)
DOI: 10.1016/j.ijengsci.2022.103672

**Abstract**

Elastic–plastic bending of microstructure-dependent beams is analyzed, i.e., beams whose external dimensions and characteristic internal length are close. The formulations presented concern space-fractional Euler–Bernoulli (s-FEBB) and Timoshenko (s-FTB) beams, enriched by including the plastic properties of the material. The Huber–Mises–Hencky plasticity criterion and isotropic hardening are applied in the developed models. The incremental iterative numerical procedure is elaborated to solve the elastic–plastic bending problem. The analysis covers not only the scale effect but also the grain size-dependent strengthening described by the general Hall–Petch relation. Based on the experimental results of WC-Co micropillars compression available in the literature, model parameters are identified for specific microstructures. Significant results were found — it was revealed that the length scale could be directly correlated with the grain size. Finally, a numerical study of elastic–plastic bending of a fractional beam demonstrated how the microstructure affects the propagation of plastic hinges.

## A.5 Publication 5

**P. Stempin**, T. P. Pawlak and W. Sumelka. *Formulation of non-local space-fractional plate model and validation for composite micro-plates* International Journal of Engineering Science, 2023, 192, 103932. ($IF_{2022} = 6.600$)
DOI: 10.1016/j.ijengsci.2023.103932

**Abstract**

It is challenging to design nano/micro-devices because of their small size and tight engineering tolerances. Computer-aided design uses mathematical models of device parts, but contemporary models are not precise enough to capture all characteristics of the materials at the nano/micro-scale. In this work, we propose a novel mathematical model for composite nano/micro-plates in bending in the framework of a space-fractional continuum mechanics approach. This model yields closer mapping of experimental results compared to existing formulations. The developed theory is named the space-Fractional Kirchhoff–Love Plate (s-FKLP). We investigate how the parameters of the s-FKLP model, responsible for the scale effect description, affect the bending behavior of the micro-plates, considering different support conditions. In addition, we compare the results predicted by s-FKLP with the previously developed simpler (one-dimensional) space-Fractional Euler–Bernoulli Beam (s-FEBB) model to show that the choice of structural analysis strategy can influence design decisions. Despite its greater complexity, the s-FKLP is a more versatile approach to modeling micro-sized structures than the s-FEBB. The proposed s-FKLP model is empirically validated using real sandwich micro-plates. We conclude model alignment with the experimental data indicating that the model is suitable for representing sandwich micro-plates. We also find that the model's length scale parameter corresponds to the microstructure's grain size. The findings of this research may have implications for future work in the design and optimization of micro-sized devices.

# B

# Co-autor's statements

POZNAN UNIVERSITY OF TECHNOLOGY

mgr inż. Paulina Stempin

FACULTY OF CIVIL AND TRANSPORT ENGINEERING
INSTITUTE OF STRUCTURAL ANALYSIS
Piotrowo 5 Street, 60-965 Poznań
e-mail: paulina.stempin@put.poznan.pl

**Poznań, 09.10.2023**

**STATEMENT OF MAIN CONTRIBUTION TO SCIENTIFIC PUBLICATIONS**

I declare that I am the first and main author in the following scientific publications:

1. **P. Stempin** and W. Sumelka. *Space-fractional Euler-Bernoulli beam model - Theory and identification for silver nanobeam bending*. International Journal of Mechanical Sciences, 2020, 186, 105902. DOI: 10.1016/j.ijmecsci.2020.105902

   My participation included defining the governing equation of the space-Fractional Euler-Bernoulli Beam (s-FEBB) theory for static elastic bending; developing the numerical model and its implementation; analyzing the effect of the new model parameters on the static response of the beam in bending; identifying the model parameters for silver nano-beams; validating the model; analysis and interpretation of results; preparation of the figures; preparing and writing the manuscript.

2. **P. Stempin** and W. Sumelka. *Formulation and experimental validation of space-fractional Timoshenko beam model with functionally graded materials effects*. Computational Mechanics, 2021, 68, 697-708. DOI: 10.1007/s00466-021-01987-6

   My participation included defining the governing equation of the space-Fractional Timoshenko Beam (s-FTB) theory for static elastic bending; developing the numerical model and its implementation; analyzing the effect of the new model parameters on the static response of the beam in bending; comparison of the results obtained according to s-FTB and s-FEBB models; identifying the model parameters for SU-8 micro-cantilevers; validating the model; analysis and interpretation of results; preparation of the figures; preparing and writing the manuscript.

3. **P. Stempin** and W. Sumelka. *Dynamics of Space-Fractional Euler–Bernoulli and Timoshenko Beams*. Materials, 2021, 14, 1817. DOI: 10.3390/ma14081817

   My participation included defining the governing equations of the s-FEBB and s-FTB theories for free vibrations; developing the numerical model and its implementation; analyzing the effect of the new model

POZNAN UNIVERSITY OF TECHNOLOGY

mgr inż. Paulina Stempin

FACULTY OF CIVIL AND TRANSPORT ENGINEERING
INSTITUTE OF STRUCTURAL ANALYSIS
Piotrowo 5 Street, 60-965 Poznań
e-mail: paulina.stempin@put.poznan.pl

parameters on the eigenvalues and eigenmodes of the beams; comparison of the results obtained according to s-FTB and s-FEBB models; identifying the model parameters for GaN nano-beams; validating the model; analysis and interpretation of results; preparation of the figures; preparing and writing the manuscript.

4. **P. Stempin** and W. Sumelka. *Space-fractional small-strain plasticity model for microbeams including grain size effect*. International Journal of Engineering Science, 2022, 175, 103672.
DOI: 10.1016/j.ijengsci.2022.103672

   My participation included defining the governing equations of the s-FEBB and s-FTB theories for static elastic-plastic bending; developing the numerical model and its implementation; analyzing the effect of the new model parameters on the evolution of the plastic zones with the determination of the value of the critical load; comparison of the results obtained according to s-FTB and s-FEBB models; identifying the parameters of the 1D space-fractional model for the compression test of WC-Co micropillars; analysis and interpretation of results; preparation of the figures; preparing and writing the manuscript.

5. **P. Stempin**, T. P. Pawlak and W. Sumelka. *Formulation of non-local space-fractional plate model and validation for composite micro-plates*. International Journal of Engineering Science, 2023, 192, 103932.
DOI: 10.1016/j.ijengsci.2023.103932

   My participation included defining the governing equation of the space-Fractional Kirchhoff-Love Plate (s-FKLP) theory for static elastic bending; developing the numerical model; analyzing the effect of the new model parameters on the static response of the plate in bending; comparison of the results obtained according to s-FKLP and s-FEBB models; identifying the model parameters for composite micro-plates; validating the model; analysis and interpretation of results; preparation of the figures; preparing and writing the manuscript.

Signed by / Podpisano przez:
Paulina Anna Stempin
Date / Data: 2023-10-09 11:16
Signature

Signed by / Podpisano przez:
Wojciech Ludwik Sumelka
Politechnika Poznańska
Date / Data: 2023-10-09 14:11
Supervisor confirmation

POZNAN UNIVERSITY OF TECHNOLOGY

prof. dr hab. inż. Wojciech Sumelka

FACULTY OF CIVIL AND TRANSPORT ENGINEERING
INSTITUTE OF STRUCTURAL ANALYSIS
Piotrowo 5 Street, 60-965 Poznań, tel.: +48 61 647 59 23
e-mail: wojciech.sumelka@put.poznan.pl

**Poznań, 09.10.2023**

## STATEMENT OF CONTRIBUTION TO SCIENTIFIC PUBLICATIONS

I declare that I have actively participated in the preparation of the following scientific publications:

1. P. Stempin and **W. Sumelka**. *Space-fractional Euler-Bernoulli beam model - Theory and identification for silver nanobeam bending*. International Journal of Mechanical Sciences, 2020, 186, 105902.
   DOI: 10.1016/j.ijmecsci.2020.105902
2. P. Stempin and **W. Sumelka**. *Formulation and experimental validation of space-fractional Timoshenko beam model with functionally graded materials effects*. Computational Mechanics, 2021, 68, 697-708.
   DOI: 10.1007/s00466-021-01987-6
3. P. Stempin and **W. Sumelka**. *Dynamics of Space-Fractional Euler–Bernoulli and Timoshenko Beams*. Materials, 2021, 14, 1817.
   DOI: 10.3390/ma14081817
4. P. Stempin and **W. Sumelka**. *Space-fractional small-strain plasticity model for microbeams including grain size effect*. International Journal of Engineering Science, 2022, 175, 103672.
   DOI: 10.1016/j.ijengsci.2022.103672
5. P. Stempin, T. P. Pawlak and **W. Sumelka**. *Formulation of non-local space-fractional plate model and validation for composite micro-plates*. International Journal of Engineering Science, 2023, 192, 103932.
   DOI: 10.1016/j.ijengsci.2023.103932

My participation in the preparation of the above scientific publications included the conception of the research; substantive supervision; discussion of the results obtained with critical analysis; writing a part of the manuscript; review and editing of the manuscripts; acquisition of financial support for the project leading to the publications 1-4. As a supervisor of the doctoral student, I acted as a corresponding author. At the same time, I state that Paulina Stempin is the main author of the aforementioned publications.

Signed by / Podpisano przez:
Wojciech Ludwik Sumelka
Politechnika Poznańska
Date / Data: 2023-10-09 14:12

POZNAN UNIVERSITY OF TECHNOLOGY

dr hab. inż. Tomasz P. Pawlak

FACULTY OF COMPUTING AND TELECOMMUNICATIONS
INSTITUTE OF COMPUTING SCIENCE
Piotrowo 2 Street, 60-965 Poznań, tel.: +48 61 665 30 22
e-mail: tomasz.pawlak@put.poznan.pl

**Poznań, 09.10.2023**

## STATEMENT OF CONTRIBUTION TO SCIENTIFIC PUBLICATION

I declare that I have actively participated in the preparation of the following scientific publication:

1. P. Stempin, **T. P. Pawlak** and W. Sumelka. *Formulation of non-local space-fractional plate model and validation for composite micro-plates*. International Journal of Engineering Science, 2023, 192, 103932. DOI: 10.1016/j.ijengsci.2023.103932

My participation in the preparation of the above scientific publication included the implementation of the numerical model; writing a part of the manuscript; revision and editing of the manuscript. I agree to use the above-mentioned publication in the dissertation of Paulina Stempin.


Signature



Poznan University of Technology
Faculty of Civil and Transport Engineering
Institute of Structural Analysis

Typeset using LaTeX